

Self-consistent model of confinement

Arthur R. Swift

Department of Physics and Astronomy, University of Massachusetts, Amherst, Massachusetts 01003

(Received 17 November 1986; revised manuscript received 27 August 1987)

A model of the large-spatial-distance, zero-three-momentum, limit of QCD is developed from the hypothesis that there is an infrared singularity. Single quarks and gluons do not propagate because they have infinite energy after renormalization. The Hamiltonian formulation of the path integral is used to quantize QCD with physical, nonpropagating fields. Perturbation theory in the infrared limit is simplified by the absence of self-energy insertions and by the suppression of large classes of diagrams due to vanishing propagators. Remaining terms in the perturbation series are resummed to produce a set of nonlinear, renormalizable integral equations which fix both the confining interaction and the physical propagators. Solutions demonstrate the self-consistency of the concepts of an infrared singularity and nonpropagating fields. The Wilson loop is calculated to provide a general proof of confinement. Bethe-Salpeter equations for quark-antiquark pairs and for two gluons have finite-energy solutions in the color-singlet channel. The choice of gauge is addressed in detail. Large classes of corrections to the model are discussed and shown to support self-consistency.

I. INTRODUCTION

This paper describes an analytic model of confinement in quantum chromodynamics (QCD). Like all such calculations, a specific mechanism for the confinement process is proposed. However, the model differs from others¹ in its reliance on the equations of QCD, the requirement of self-consistency, and the ability to analyze corrections. Radical hypotheses about the nature of certain vacuum expectation values (VEV's) are acceptable *only* if they are consistent with the field equations and are stable against corrections. The result of this investigation is a "theory" in which colored states have infinite energy, there exists a Bethe-Salpeter equation for finite-energy color-singlet bound states, and residual interactions are calculable with simplified perturbation theory rules. The paper is devoted to an exposition of the model, its strengths, and its defects. The goal is not to present the ultimate theory of confinement, but rather to explore one possible mechanism and develop it to the point where it can be used to discuss interesting problems in bound-state physics wholly within the framework of QCD. Emphasis is always on the low-three-momentum, large-spatial-distance limit. Some of the results have appeared in a series of papers on the connection between the QCD vacuum and confinement.²⁻⁴ The derivation here is totally new, almost rigorous, and self-contained.

The self-consistent model is formulated in the Coulomb gauge. The problems of the Coulomb gauge are well known.⁵ However, it is the natural gauge in which to discuss bound states,^{6,7} and it is well matched to the treatment of the small-three-momentum limit. Two key hypotheses define this model. There is a singularity at zero three-momentum (the infrared limit) in the QCD version of the instantaneous Coulomb interaction. The singularity is controlled by a cutoff parameter and is responsible for the long-range, confining interaction. The second hy-

pothesis is that quarks and transverse gluons do not propagate in the physical vacuum because they have infinite energy. The energy depends on the infrared cutoff parameter and becomes infinite as the cutoff is removed. A consequence of this hypothesis is that perturbation theory in the physical vacuum is simplified. Feynman diagrams with more than one gluon and/or quark in a momentum loop vanish as the cutoff is removed. Surviving diagrams are summed to generate a set of nonlinear integral equations for effective propagators and for the Coulomb interaction. Even though the emphasis is on the zero-momentum limit, the equations are renormalizable. Solutions exist which are consistent with the hypothesized singularity structure. *The model is self-consistent; the hypotheses are justified a posteriori.* Moreover, screening effects produced by quark and gluon pairs do not alter the conclusions. It is hard to create infinite-energy particles out of the vacuum. The Wilson loop⁸ is calculable and verifies confinement. Color-singlet bound states exist in both the quark and gluon sectors. A linear potential is favored. This model, like the simple MIT bag model,⁹ confines quarks and gluons by the same mechanism, contrary to indications from lattice calculations which suggest that quarks are confined and gluons are screened.

The model starts with the Coulomb-gauge Hamiltonian of Christ and Lee.¹⁰ Problems with zeros of the Faddeev-Popov¹¹ determinant are sidestepped by use of the Hamiltonian formulation of path-integral quantization.¹² Terms are added and subtracted to define a free-particle action that is quadratic in "physical" fields and their conjugate momenta.¹³ By coupling external sources to fields and momenta one derives effective propagators. The interaction Hamiltonian is also a function of both fields and momenta.⁷ Not only does the Faddeev-Popov determinant not appear, but there is no need for ghost fields. A complication is the appearance of interactions which are nonlocal and of all order in the coupling con-

stant. However, there are anomalous interactions in the Coulomb gauge which have an equally complicated structure.^{10,14}

A gauge-invariant, Lorentz-invariant theory of confinement would be far preferable to one based on the Coulomb gauge. Such a model has yet to appear. The Coulomb gauge is unique in that only the physical degrees of freedom of the gauge field are quantized. It is precisely those transverse gluons which do not propagate as normal particles. In addition, the Coulomb gauge has the virtue that the QCD version of Gauss's law does not need to be imposed as a separate condition on states.¹⁰ Thus, only in the Coulomb gauge does it make sense to treat a meson as a bound state of a quark and an antiquark. In other gauges one needs a gauge-dependent phase factor that involves the gluon field and, therefore, an indefinite number of gluons. Although the Coulomb gauge has been frequently used in bound-state calculations,^{6,7} problems associated with the lack of Lorentz invariance, the need for anomalous interactions, and the zeros of the Faddeev-Popov determinant¹⁵ have been generally ignored. The virtues of the Coulomb gauge must not obscure the possibility that in any incomplete calculation the results might be an artifact of the choice of gauge.

Lorentz invariance is a problem because the condition $\nabla \cdot \mathbf{A} = 0$ singles out a particular frame. It is possible to define boost operators that transform states and operators to an arbitrary frame,¹⁶ or one can construct a covariant Coulomb gauge. An arbitrary timelike vector η^μ [$\eta \cdot \eta = (\eta^0)^2 - \boldsymbol{\eta} \cdot \boldsymbol{\eta} = 1$] defines a time parameter $\tau = \eta \cdot x$. Quantization on a surface of constant τ with the gauge condition $\partial \cdot A - \eta \cdot \partial \eta \cdot A = 0$ produces a set of equivalent theories in which $\eta \cdot A$ carries a τ instantaneous interaction. For each η there is a confining theory, but it is not obvious that these η Coulomb gauges are equivalent to each other. The ground states are certainly not identical. On the other hand, since QCD is gauge invariant, covariant and noncovariant gauges are equivalent if gauge-invariant amplitudes are calculated to all orders in the coupling constant. In the present model, perturbation theory is simplified by the nonpropagation of quarks and gluons. It is possible to calculate the effects of large classes of diagrams and restore a measure of Lorentz invariance.

It is appropriate to ask whether one should demand Lorentz invariance in a theory of confinement, a low-three-momentum, large-spatial-distance phenomenon. The description of a meson as a quark-antiquark pair connected by a flux tube is certainly neither covariant nor invariant. If a two-particle state is boosted, an indefinite number of "sea" particles are created. Any model of hadrons formed from a finite number of constituents necessarily lacks Lorentz invariance and is restricted to low momentum.

Singularities due to the vanishing of the Faddeev-Popov determinant^{15,17} do not appear in the quantization method adopted here. The determinant is buried implicitly in the state vectors. Christ and Lee¹⁰ recover covariant Feynman rules in the Coulomb gauge while ignoring wave-function singularities. Quantization about

the physical vacuum also suppresses the large field components which occur at zero momentum in ordinary perturbation theory. The Faddeev-Popov determinant is well behaved for weak fields.¹⁷ The philosophy of this paper is that singularities arise as a result of dynamics. Perturbation theory is defined for weak, physical fields. Series are resummed and analytically continued to find singularities.

Is the whole calculation a gauge artifact? A hidden hypothesis is that one gauge is favored over all others for analysis of the zero-momentum limit of QCD (Ref. 18). Such a favored gauge will not be covariant. Few-particle bound states should make sense. Although the spectrum of bound states is gauge invariant, most of the key functions (such as the gluon propagator) are not gauge invariant. Since trouble can arise when calculations are truncated to finite order, it is important to calculate large classes of diagrams to all orders and to estimate the effect of excluded diagrams. The standard test of a gauge theory calculation is consistency with the Ward identities. In this model one can ask whether the hypothesized pattern of infrared singularities passes that test. There is no easy answer. The standard derivations of Ward identities are tied to Lagrangian path-integral quantization in covariant gauges,¹⁹ not the Hamiltonian formalism adopted here. Derivations assume an invariant vacuum state. The Christ and Lee prescription for quantization in the Coulomb gauge includes absorbing the square root of the Faddeev-Popov determinant into the definition of states.¹⁰ Another aspect of Ward identities is that they relate longitudinal components of vertex functions to particle propagators. In the Coulomb gauge the longitudinal components of vertex functions are decoupled from the theory. The gauge fields are transverse. The nature of Ward identity constraints is an interesting question, worthy of a separate investigation, but is beyond the scope of this paper. The goal of this work is to create a model that is not in conflict with QCD, yet is simple enough to be used in the investigation of important theoretical questions related to the interplay between constituent and bound-state degrees of freedom. Unlike bag models, potential models, condensate models,¹ etc., this model is complete. Hadrons are poles in the color-singlet channel of two-particle Green's functions. Techniques exist for extracting hadronic amplitudes from quark processes. Whether QCD confinement actually is a result of the proposed set of infrared singularities is not of overwhelming importance. What matters is that the mechanism is at least consistent with QCD.

The Hamiltonian approach to path-integral quantization about the physical vacuum is developed in the next section. The result is a set of effective propagators for dressed quarks and gluons and a description of their interactions. The gauge group is $SU(N)$. Where approximations are necessary, amplitudes which do not vanish in the $N \rightarrow \infty$ limit, $g^2 N$ -fixed limit are expected to dominate.²⁰ Self-consistency is discussed in Sec. III. Some of the results have been obtained before by less reliable techniques. The Wilson loop is calculated in Sec. IV. Not only does the result display confinement, but the calculation emphasizes the significance of nonpropagating

gluons and the instantaneous, singular Coulomb interaction. Bethe-Salpeter equations for bound states are treated in Sec. V. The energy spectrum is not calculated. Corrections to the simplest version of the model are dis-

cussed in Sec. VI. Section VIII touches on possible defects and mentions applications. The numerous appendixes are devoted to important technical details.

II. QUANTIZATION IN THE COULOMB GAUGE

The QCD Hamiltonian in the Coulomb gauge is¹⁰

$$\begin{aligned}
 H = & \frac{1}{2} \int d^3r B_i^a(\mathbf{r}) B_i^a(\mathbf{r}) + \frac{1}{2} \int d^3r P_i^a(\mathbf{r}) P_i^a(\mathbf{r}) + \int d^3r \bar{\psi}_\alpha(\mathbf{r}) \left[-i\boldsymbol{\gamma} \cdot \nabla - g\boldsymbol{\gamma} \cdot \mathbf{A}^a(\mathbf{r}) \frac{\lambda^a}{2} + m \right]_{\alpha\beta} \psi_\beta(\mathbf{r}) \\
 & + \frac{g^2}{2} \int d^3r d^3r' \left[\left[f_{abc} \mathbf{P}^b(\mathbf{r}) \cdot \mathbf{A}^c(\mathbf{r}) - \bar{\psi}(\mathbf{r}) \gamma^0 \frac{\lambda^a}{2} \psi(\mathbf{r}) \right] F_{aa'}(\mathbf{r}, \mathbf{r}') \left[f_{a'b'c'} \mathbf{P}^{b'}(\mathbf{r}') \cdot \mathbf{A}^{c'}(\mathbf{r}') - \bar{\psi}(\mathbf{r}') \gamma^0 \frac{\lambda^{a'}}{2} \psi(\mathbf{r}') \right] \right]_{\mathcal{W}} \\
 & + V_1(A) + V_2(A). \tag{2.1}
 \end{aligned}$$

Both the gluon field $A_j^a(\mathbf{r})$ and its conjugate momentum field $P_i^a(\mathbf{r})$ are divergence-free in the Coulomb gauge:

$$\nabla \cdot \mathbf{A}^a = \nabla \cdot \mathbf{P}^a = 0. \tag{2.2}$$

Implicit in the definition of the quark fields $\psi_\alpha(\mathbf{r})$ are color, flavor, and Dirac indices. The quark mass matrix m is diagonal in flavor space. The gauge group is $SU(N)$, and f_{abc} represents the usual set of antisymmetry structure constants. The $N \times N$ Hermitian matrices λ^a satisfy

$$[\lambda^a, \lambda^b] = 2if_{abc} \lambda^c, \tag{2.3a}$$

$$\text{tr}(\lambda^a \lambda^b) = 2\delta_{ab}. \tag{2.3b}$$

The color-magnetic field is

$$B_i^a = \frac{1}{2} \epsilon_{ijk} (\nabla_j A_k^a - \nabla_k A_j^a + gf_{abc} A_j^b A_k^c). \tag{2.4}$$

To lowest order in the coupling constant g , $F_{aa'}(\mathbf{r}, \mathbf{r}'; t)$ is proportional to $\delta_{aa'}/|\mathbf{r} - \mathbf{r}'|$. Hence, $F_{aa'}(\mathbf{r}, \mathbf{r}'; t)$ incorporates the QCD modifications of the ordinary instantaneous Coulomb interaction of quantum electrodynamics. This modified Coulomb potential is defined by^{2,10}

$$F_{aa'}(\mathbf{r}, \mathbf{r}'; t) = \int d^3r'' D_{ab}(\mathbf{r}, \mathbf{r}''; t) (-\nabla^2) D_{ba'}(\mathbf{r}'', \mathbf{r}'; t), \tag{2.5}$$

where $D_{ab}(\mathbf{r}, \mathbf{r}'', t)$ is the modified Coulomb Green's function:

$$-[\nabla^2 \delta_{ac} + gf_{abc} \mathbf{A}^b(\mathbf{r}) \cdot \nabla] D_{cd}(\mathbf{r}, \mathbf{r}'; t) = \delta_{ad} \delta^3(\mathbf{r} - \mathbf{r}'). \tag{2.6}$$

The \mathcal{W} subscript around the Coulomb term in the Hamil-

tonian indicates Weyl ordering of the factors inside the large square brackets. Since $A_i^a(\mathbf{r})$ and $P_i^a(\mathbf{r})$ are non-commuting operators, it is necessary to specify their ordering in the quantum Hamiltonian. The final terms in (2.1), $V_1(A)$ and $V_2(A)$, are the anomalous interactions. They are absent when QCD is quantized directly in the Coulomb gauge rather than transformed from a well-behaved gauge.²¹ Explicit expressions for $V_1(A)$ and $V_2(A)$ appear in Appendix A.

Feynman rules in the Coulomb gauge are calculated from the generating function

$$W = \bar{N} \int D(A_i^a) D(P_j^b) D(\bar{\psi}_\alpha) D(\psi_\beta) \exp(iS[A, P, \psi, \bar{\psi}]), \tag{2.7}$$

when it is augmented by terms coupling fields to external sources. The integral in (2.7) involves only the physical components of the gluon field. There are no additional gauge constraints in the integrand. Since H is quadratic in momentum fields $P_i^a(\mathbf{r})$, it is conventional to explicitly carry out the momentum integrations. The result is the appearance of the Faddeev-Popov determinant and the need for ghost fields.¹⁰ An alternative method of quantization is to treat $A_i^a(\mathbf{r})$ and $P_i^a(\mathbf{r})$ as equivalent fields.⁷ First, however, I switch from configuration space to momentum space:

$$A_i^a(\mathbf{r}, t) = \int d^4k e^{-ik_0 t + i\mathbf{k} \cdot \mathbf{r}} A_i^a(k). \tag{2.8}$$

The momentum field and the quark fields are similarly transformed. That portion of the action in (2.7) which is linear or quadratic in fields is

$$\begin{aligned}
 S_0 = & -(2\pi)^4 \int d^4k d^4p \delta^4(p+k) \\
 & \times (ip_0 \mathbf{P}^a(k) \cdot \mathbf{A}^a(p) + \frac{1}{2} \mathbf{P}^a(k) \cdot \mathbf{P}^a(p) [1 + F_1(k)] + \frac{1}{2} \mathbf{A}^a(k) \cdot \mathbf{A}^a(p) [\mathbf{k}^2 + F_2(k)] + \mathbf{A}^a(k) \cdot \mathbf{J}^a(p) + \mathbf{P}^a(k) \cdot \mathbf{K}^a(p) \\
 & - \bar{\psi}(k) \gamma^0 p_0 \psi(p) + \bar{\psi}(k) \{ \boldsymbol{\gamma} \cdot \mathbf{p} [1 + G_1(p)] + m [1 + G_2(p)] \} \psi(p) + \bar{\psi}(k) \eta(p) + \bar{\eta}(k) \psi(p)). \tag{2.9}
 \end{aligned}$$

Since both $A_i^a(k)$ and $P_i^a(k)$ are transverse, only the transverse components of the external boson sources $J_i^a(k)$ and $K_i^a(k)$ are coupled. Thus, $\mathbf{J} \cdot \mathbf{A}$ is shorthand for $J_i P_{ij} A_j$ where $P_{ij}(k) = \delta_{ij} - k_i k_j / k^2$. The treatment of quark degrees of freedom is standard; η and $\bar{\eta}$ are quark source terms. The functions $F_1(k)$ and $F_2(k)$ turn bare gluon propagators into fully dressed propagators, and $G_1(k)$ and $G_2(k)$ do the same for the quark propagator. These functions are fixed by the requirement that they sum exactly all self-energy diagrams.¹³ In principle additional terms such as $i p_0 \mathbf{P}^a(k) \cdot \mathbf{A}^a(p) F_3(k)$ and $\bar{\psi}(k) \gamma^0 p_0 \Psi(p) G_3(k)$ are needed. However, self-consistency in the $\mathbf{k} \rightarrow 0$ limit does not require them. The terms added to make S_0 the action for particles propagating in the physical vacuum are compensated for by the subtraction of identical quadratic terms in the interaction Hamiltonian.

The standard path-integral formalism yields the following effective single-gluon propagators:

$$\langle A_i^a(k) A_j^b(p) \rangle = \frac{i}{(2\pi)^4} \delta_{ab} \delta^4(p+k) P_{ij}(\mathbf{k}) \frac{1+F_1(k)}{d(k)}, \quad (2.10a)$$

$$\langle P_i^a(k) P_j^b(p) \rangle = \frac{i}{(2\pi)^4} \delta_{ab} \delta^4(p+k) P_{ij}(\mathbf{k}) \frac{k^2+F_2(k)}{d(k)}, \quad (2.10b)$$

$$\langle P_i^a(k) A_j^b(p) \rangle = \frac{i}{(2\pi)^4} \delta_{ab} \delta^4(p+k) P_{ij}(\mathbf{k}) \frac{i k_0}{d(k)}, \quad (2.10c)$$

where

$$d(k) = k_0^2 - [k^2 + F_2(k)][1 + F_1(k)] + i\epsilon = k_0^2 - \omega(k)^2 + i\epsilon. \quad (2.11)$$

The transverse projection operators arise from the fact that only the transverse components of the vector sources occur. The quark propagator is

$$\langle \psi_\alpha(p) \bar{\psi}_\beta(k) \rangle = \frac{i}{(2\pi)^4} \delta^4(p+k) \frac{\{-\gamma^0 k_0 + \boldsymbol{\gamma} \cdot \mathbf{k} [1 + G_1(k)] + m [1 + G_2(k)]\}_{\alpha\beta}}{d_F(k)} \quad (2.12)$$

with

$$d_F(p) = p_0^2 - \mathbf{p}^2 [1 + G_1(p)]^2 - m^2 [1 + G_2(p)]^2 + i\epsilon. \quad (2.13)$$

If the functions F_1 , F_2 , G_1 , and G_2 contain terms which become infinite in the infrared limit, then the poles in the propagators are shifted to $k_0 = \pm \infty$.

Interactions are described by $S_I = \int H_I(A, P, \Psi, \bar{\Psi}) dt$. In momentum space this becomes

$$\begin{aligned} S_I(A, P, \psi, \bar{\psi}) = & (2\pi)^4 \int d^4 P d^4 k \delta^4(p+k) \left\{ \frac{1}{2} \mathbf{P}^a(p) \cdot \mathbf{P}^a(k) F_1(k) + \frac{1}{2} \mathbf{A}^a(p) \cdot \mathbf{A}^a(k) F_2(k) + \bar{\psi}(p) [\boldsymbol{\gamma} \cdot \mathbf{k} G_1(k) + m G_2(k)] \psi(k) \right\} \\ & - ig (2\pi)^4 f_{abc} \int d^4 1 d^4 2 d^4 3 \delta^4(1+2+3) \mathbf{A}^a(1) \cdot \mathbf{A}^c(3) \mathbf{1} \cdot \mathbf{A}^b(2) \\ & - \frac{g^2}{4} (2\pi)^4 f_{abc} f_{ade} \int d^4 1 d^4 2 d^4 3 d^4 4 \delta^4(1+2+3+4) \mathbf{A}^b(1) \cdot \mathbf{A}^d(3) \mathbf{A}^c(2) \cdot \mathbf{A}^e(4) \\ & + \frac{g}{2} (2\pi)^4 \int d^4 1 d^4 2 d^4 3 \bar{\psi}(1) \boldsymbol{\gamma} \cdot \mathbf{A}^a(3) \lambda^a \psi(2) \delta^4(1+2+3) - \int dt [V_1(A) + V_2(A)] \\ & - \frac{g^2}{2} (2\pi)^7 \int d^4 1 d^4 2 d^4 3 d^4 4 dx \delta(1_0+2_0+3_0+4_0+x) \\ & \quad \times [f_{abc} \mathbf{P}^b(1) \cdot \mathbf{A}^c(2) - \frac{1}{2} \bar{\psi}(1) \boldsymbol{\gamma}^0 \lambda^a \psi(2)] F_{aa'}(-1-2, -3-4; x) \\ & \quad \times [f_{a'de} \mathbf{P}^d(3) \cdot \mathbf{A}^e(4) - \frac{1}{2} \bar{\psi}(3) \boldsymbol{\gamma}^0 \lambda^{a'} \psi(4)]. \end{aligned} \quad (2.14)$$

Explicit expressions for the anomalous interaction terms are given in Appendix A. Except for the restriction to spatial components, the three-gluon, four-gluon, and quark-quark-gluon terms are standard QCD interactions. The final term in (2.14) is the modified Coulomb interaction. The modified Coulomb operator has the Fourier transform

$$F_{aa'}(\mathbf{r}, \mathbf{r}'; t) = \int d^3 p d^3 k dx e^{-ixt} e^{i\mathbf{p} \cdot \mathbf{r}} e^{i\mathbf{k} \cdot \mathbf{r}'} F_{aa'}(\mathbf{p}, \mathbf{k}; x). \quad (2.15)$$

It will be necessary to calculate this function from its definition in terms of the modified Coulomb Green's function $D_{ab}(\mathbf{r}, \mathbf{r}'; t)$. If the Green's function has a Fourier transform such as (2.15), then

$$F_{aa'}(\mathbf{p}, \mathbf{k}; x) = (2\pi)^3 \int d^3 s dy dz D_{ab}(\mathbf{p}, \mathbf{s}; y) s^2 D_{ba'}(-\mathbf{s}, \mathbf{k}; z) \delta(x-y-z). \quad (2.16)$$

The differential equation (2.6) becomes an integral equation in momentum space:

$$D_{ab}(\mathbf{p}, \mathbf{k}; x) = \frac{\delta_{ab} \delta^3(\mathbf{p} + \mathbf{k}) \delta(x)}{(2\pi)^3 \mathbf{p}^2} + igf_{ace} \frac{1}{\mathbf{p}^2} \int d^4s \mathbf{A}^c(s) \cdot \mathbf{p} D_{eb}(\mathbf{p} - \mathbf{s}, \mathbf{k}; x - s_0). \quad (2.17)$$

If (2.17) is expanded in a perturbation series and the result is inserted in (2.16), one can prove that

$$F_{ab}(\mathbf{p}, \mathbf{k}; x) = \frac{d}{dg} [g D_{ab}(\mathbf{p}, \mathbf{k}; x)]. \quad (2.18)$$

In the $g=0$ limit $F_{ab}(\mathbf{p}, \mathbf{k}; x)$ is equal to the first term in (2.18). More generally the Coulomb part of S_I as well as V_1 and V_2 , contains interactions of all orders in g and can lead to the creation of an arbitrarily large number of gluons.

The self-consistent theory of confinement is defined by the following set of assumptions.

(1) There is an infrared singularity in the theory that can be controlled by a cutoff parameter μ .

(2) The subtraction functions F_1, F_2, G_1, G_2 diverge as $\mu \rightarrow 0$. Each function has a term proportional to a constant $\lambda(\mu)$, where $\lambda(\mu) \rightarrow \infty$ as $\mu \rightarrow 0$.

(3) In Feynman diagrams integrations over p_0 , the time component of a loop momentum, are to be performed before setting $\mu=0$.

(4) The vacuum expectation value (VEV) of the modified Coulomb interaction has the form

$$\langle F_{ab}(\mathbf{p}, \mathbf{k}; x) \rangle = \frac{\delta_{ab} \delta^3(\mathbf{p} + \mathbf{k}) \delta(x)}{(2\pi)^3} F(\mathbf{p}), \quad (2.19)$$

where, as $\mu \rightarrow 0$, the function $F(\mathbf{p})$ develops a singularity at $\mathbf{p}=0$. The structure of the VEV is fixed by symmetry requirements, except for the unknown function $F(\mathbf{p})$. The singularity in this function is such that in any integral involving $F(\mathbf{p})$, one can set

$$F(\mathbf{p}) = \lambda(\mu) \delta^3(\mathbf{p}) + \bar{F}(\mathbf{p})$$

and the effects of the singularity are totally absorbed in $\lambda(\mu)$.

These assumptions are shown to be self-consistent in the next section. The vacuum expectation values of $F_{ab}(\mathbf{p}, \mathbf{k}; x)$ and $D_{ab}(\mathbf{p}, \mathbf{k}; k)$ play a prominent role as the effective propagators for the Coulomb interaction.

Hypotheses (1) and (2) imply that at fixed momentum all single-particle propagators vanish in the $\mu=0$ limit. For example, the $\langle AA \rangle$ propagator for gluons becomes proportional to $F_1/(F_1 F_2) \rightarrow \lambda^{-1} \rightarrow 0$ when $F_1 \gg 1$ and $F_2 \gg k^2$. Moreover, the pole in the k_0 plane moves to $k_0 = \pm(F_1 F_2)^{1/2} \rightarrow \pm \lambda \rightarrow \pm \infty$ as $\mu \rightarrow 0$. If a propagator occurs inside a momentum loop, there are, according to (3), contributions from encircling the k_0 poles. The residue of the pole of an $\langle AA \rangle$ propagator is proportional to $F_1/(F_1 F_2)^{1/2} \simeq \lambda^0$. The residue is finite at $\mu=0$. Thus, a momentum loop with a single quark or gluon line (and a number of instantaneous Coulomb lines) has a finite infrared limit. In general, each momentum integration encircles a pole and compensates for one factor of λ^{-1} . Quark lines are treated in the same way. Diagrams with two or more gluons and/or quarks in a momentum loop vanish in the infrared limit. For n particles, a momentum loop is of order λ^{1-n} . In addition, the interactions in (2.14) never produce a momentum loop

composed entirely of Coulomb lines. As a result there are no spurious divergences from k_0 integrations.

By hypothesis the propagator of the Coulomb interaction is singular and produces a positive power of the divergent parameter λ . Hence, finite amplitudes can occur when vanishing propagators are compensated by either momentum integrations or singular Coulomb propagators. If the Feynman diagram for a particular process contains L momentum loops, G gluon propagators (of any type), Q quark propagators, and C singular Coulomb propagators, the amplitude will be proportional to λ^M where, as shown in Appendix C,

$$M = 1 - n_{gggg} - n_{qqg} - n_{ggg}. \quad (2.20)$$

The maximum value of M is 1, and it occurs when there are no four-gluon vertices ($n_{gggg}=0$), three-gluon vertices ($n_{ggg}=0$), or quark-quark-gluon vertices ($n_{qqg}=0$). Diagrams with $M < 0$ vanish. An example of an $M=1$ amplitude is the set of ladder diagrams for quark-antiquark scattering via singular Coulomb exchange. (There is a constraint condition that eliminates the $M=1$ term to leave a finite function.) Diagrams with $M=1$ are also responsible for the infrared divergence in propagator functions. It is important to remember that there are no quark or gluon self-energy diagrams in the perturbation series. They are summed exactly by the use of effective propagators.

In constructing a set of Feynman rules, one must recognize that there are three separate gluon propagators corresponding to $\langle AA \rangle$, $\langle PP \rangle$, and $\langle AP \rangle$, and two Coulomb propagators which are distinguished by their behavior at $\mathbf{p}=0$. The VEV of the modified Coulomb interaction is singular in that limit, while the second propagator is the nonsingular VEV of the Green's function. The Green's-function propagator is needed to describe the multigluon interactions inherent in the Coulomb, V_1 , and V_2 contributions to S_I .

III. SELF-CONSISTENCY

The amplitudes corresponding to Feynman diagrams depend on six unknown functions—four functions in the effective propagators and the Coulomb functions $F(\mathbf{p})$ and $D(\mathbf{p})$. The model makes sense only if these functions can be calculated nonperturbatively. The simplest function to analyze is the VEV of the modified Green's function. The perturbation expansion of $D_{ab}(\mathbf{p}, \mathbf{k}; x)$ is given in (B1) of Appendix B. The VEV of D_{ab} has the diagrammatic representation of Fig. 1. Diagrams which vanish in the $\lambda \rightarrow \infty$ limit have been eliminated. The only nonvanishing diagrams are those in which physical gluons are emitted and reabsorbed by the gluon line. The perturbation series for this subset can be resummed to produce a Dyson equation for the unknown function in $\langle D_{ab} \rangle$:

$$D(\mathbf{k}) = \frac{1}{\mathbf{k}^2} \frac{1}{1 - gI(\mathbf{k})}, \quad (3.1)$$

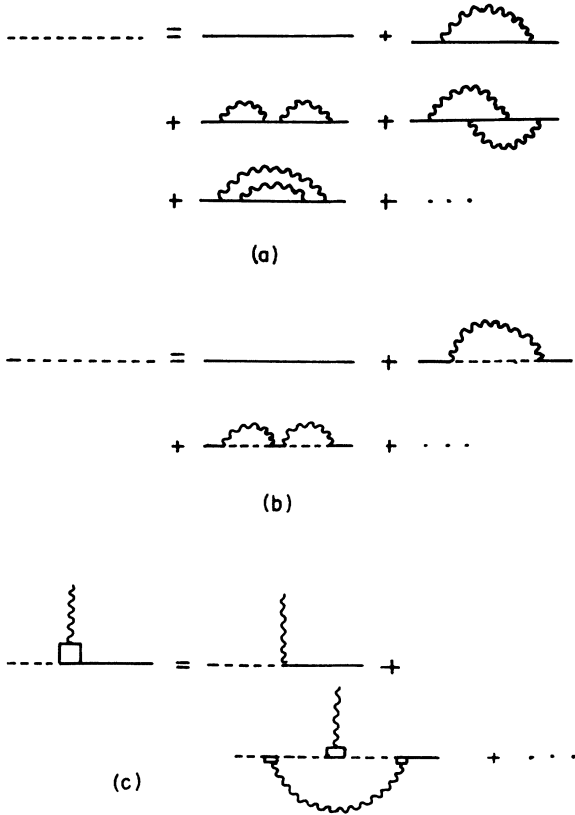


FIG. 1. The perturbation series for the Coulomb Green's function is portrayed in (a). Solid lines are $1/p^2$ propagators and wavy lines are gluons. The perturbation series is resummed in (b); the dashed line is the dressed propagator function $D(p)$. The nature of the integral equation for the vertex function is shown in (c).

where $D(k)$ is defined in (B3). If the DgD_0 vertex function in Fig. 1 ($D_0=1/k^2$) is replaced by its zeroth-order value

$$I(\mathbf{k}) = \frac{N}{2(2\pi)^3} \int d^3p \frac{p^2 k^2 - (\mathbf{p} \cdot \mathbf{k})^2}{p^2 k^2} A(\mathbf{p}) g D(\mathbf{p} - \mathbf{k}) \quad (3.2)$$

for the gauge group $SU(N)$. The role of vertex corrections and other higher-order corrections is addressed in Sec. VI and Appendix E. The propagator function $A(\mathbf{p})$ is of order $\lambda^{0,4}$

$$A(\mathbf{p}) = \frac{i}{\pi} \int_{-\infty}^{\infty} dp_0 \frac{1 + F_1(\mathbf{p})}{p_0^2 - [1 + F_1(\mathbf{p})][p^2 + F_2(\mathbf{p})]} = \left[\frac{1 + F_1(\mathbf{p})}{p^2 + F_2(\mathbf{p})} \right]^{1/2} \quad (3.3)$$

I have used the fact, to be verified shortly, that $F_1(\mathbf{p})$ and $F_2(\mathbf{p})$ are independent of p_0 in the $\lambda \rightarrow \infty$ limit.

Equations (3.1) and (3.2) were derived in an earlier work on the relationship between confinement and properties of the QCD vacuum.³ The extensive discussion will not be repeated here. Asymptotic freedom predicts that, within logarithms, $A(\mathbf{p}) \rightarrow 1/p$ and $D(\mathbf{p}) \rightarrow 1/p^2$ as $\mathbf{p} \rightarrow \infty$. Renormalization is necessary to remove a loga-

rithmic divergence in (3.2). Analysis of the $\mathbf{p} \rightarrow 0$ limit shows that if $A(\mathbf{p})$ approaches a constant, $D(\mathbf{p})$ is proportional to $(p^2)^{-5/4}$. Conventional perturbation theory sets $A(\mathbf{p})=1/p$ and $D(p)=1/p^2$ in lowest order.

The $\mathbf{p}=0$ enhancement of $D(\mathbf{p})$ is promoted to a true infrared singularity in $F(\mathbf{p})=d[gD(\mathbf{p})]/dg$. Differentiation of (3.1) leads to

$$F(\mathbf{p}) = \frac{1}{p^2} \frac{1 + g^2 J(\mathbf{p})}{[1 - gI(\mathbf{p})]^2} \quad (3.4)$$

with

$$J(\mathbf{p}) = \frac{N}{2(2\pi)^3} \int d^3k \frac{p^2 k^2 - (\mathbf{p} \cdot \mathbf{k})^2}{p^2 k^2} A(\mathbf{k}) F(\mathbf{p} - \mathbf{k}) \quad (3.5)$$

These equations also appeared in the paper on the QCD vacuum.³ Since $F(\mathbf{p}) \rightarrow 1/p^2$ as $p \rightarrow \infty$, the integral defining $J(\mathbf{p})$ is logarithmically divergent. After renormalization, the solution of (3.4) must lead to an infrared singularity in $F(\mathbf{p})$ in order to satisfy the self-consistency requirement.

$F(\mathbf{p})$ is infrared singular if, as $\mathbf{p} \rightarrow 0$, $F(\mathbf{p}) \propto (p^2)^{-n}$, and $n \geq \frac{3}{2}$. When n is in the range $\frac{3}{2} \leq n < \frac{5}{2}$, the singularity can be controlled by a simple subtraction procedure. One possible parametrization is

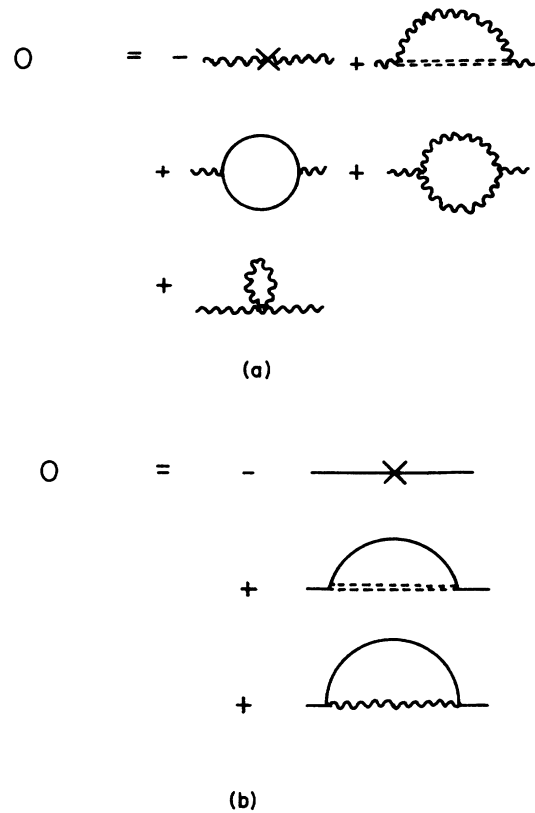


FIG. 2. The order- g^2 gluon counterterm, marked by a cross in (a), cancels four diagrams. Only the diagram with the singular Coulomb propagator indicated by a double-dashed line survives the infrared limit. Quark lines are solid. The quark counterterm equation is shown in (b).

$$F(\mathbf{p}) = \frac{f}{(p^2 + \mu^2)^n} \quad (3.6)$$

Then for an arbitrary function $H(\mathbf{k})$,

$$I(\mathbf{p}) = \int d^3k F(\mathbf{k} - \mathbf{p})H(\mathbf{k}) = \lambda(\mu)H(\mathbf{p}) + \bar{I}(\mathbf{p}) \quad (3.7)$$

The integral $\bar{I}(p)$ is finite as $\mu \rightarrow 0$ and

$$\lambda(\mu) = \frac{2\pi\Gamma(\frac{3}{2})\Gamma(n - \frac{3}{2})}{\mu^{2n-3}\Gamma(n)} \quad (3.8)$$

Equation (3.7) is equivalent to writing

$$F(\mathbf{p}) = \lambda(\mu)\delta^3(p) + \bar{F}(\mathbf{p}) \quad (3.9)$$

Integrals containing $\bar{F}(\mathbf{p})$ are defined from (3.6) with the stipulation that μ -dependent divergences are to be discarded. For example, in (3.5) $F(\mathbf{p} - \mathbf{k})$ can be replaced by $\bar{F}(\mathbf{p} - \mathbf{k})$, since $p^2k^2 - (\mathbf{p} \cdot \mathbf{k})^2$ vanishes at $\mathbf{p} = \mathbf{k}$, and the integral is finite at $\mu = 0$.

The theory is complete when $A(\mathbf{p})$ and the quark and gluon effective propagators are calculated. The sums of all self-energy insertions in gluon lines are canceled by the quadratic terms in the interaction Hamiltonian. Order- g^2 corrections to gluon and quark lines are shown in Fig. 2. Quadratic insertions are indicated by crosses. If (2.20) is correct, only the diagrams with a singular Coulomb line contribute in the $\lambda \rightarrow \infty$ limit. Other self-energy diagrams are of order λ^{-1} . The second-order correction to (2.10a) is

$$\begin{aligned} \langle A_i^a(\mathbf{k}) A_j^b(\mathbf{p}) \rangle_{g^2} &= \frac{i}{(2\pi)^4} \delta_{ab} \delta^4(\mathbf{p} + \mathbf{k}) P_{ij}(\mathbf{k}) \\ &\times \frac{1}{d(k)} \left[-k_0^2 \left[F_1(\mathbf{k}) - \frac{g^2 N}{4(2\pi)^3} \int d^3s F(\mathbf{s} - \mathbf{k}) A(\mathbf{s}) \text{tr}[P(\mathbf{s})P(\mathbf{k})] \right] \right. \\ &\quad \left. - [1 + F_1(\mathbf{k})]^2 \left[F_2(\mathbf{k}) - \frac{g^2 N}{4(2\pi)^3} \int d^3s \frac{F(\mathbf{s} - \mathbf{k})}{A(\mathbf{s})} \text{tr}[P(\mathbf{s})P(\mathbf{k})] \right] \right] \frac{1}{d(k)} \quad (3.10) \end{aligned}$$

The identical combination of F_1 , F_2 , and integrals occurs in $\langle PP \rangle$ and $\langle PA \rangle$. Hence, the condition that self-energy corrections vanish fixes F_1 and F_2 (to order g^2):

$$F_1(\mathbf{k}) = \frac{\alpha}{2} \int d^3s F(\mathbf{s} - \mathbf{k}) A(\mathbf{s}) \text{tr}[P(\mathbf{s})P(\mathbf{k})] \quad (3.11a)$$

$$F_2(\mathbf{k}) = \frac{\alpha}{2} \int d^3s F(\mathbf{s} - \mathbf{k}) \frac{1}{A(\mathbf{s})} \text{tr}[P(\mathbf{s})P(\mathbf{k})] \quad (3.11b)$$

with $\alpha = g^2 N / [2(2\pi)^3]$. The corresponding quark calculation for each flavor leads to

$$G_1(\mathbf{k}) = \frac{\alpha'}{2} \int d^3s F(\mathbf{s} - \mathbf{k}) \frac{\mathbf{k} \cdot \mathbf{s}}{k^2} \frac{1 + G_1(\mathbf{s})}{E(\mathbf{s})} \quad (3.12a)$$

$$G_2(\mathbf{k}) = \frac{\alpha'}{2} \int d^3s F(\mathbf{s} - \mathbf{k}) \frac{1 + G_2(\mathbf{s})}{E(\mathbf{s})} \quad (3.12b)$$

where $\alpha' = [(N^2 - 1)/N^2]\alpha$ and

$$E(\mathbf{s})^2 = s^2 [1 + G_1(\mathbf{s})]^2 + m^2 [1 + G_2(\mathbf{s})]^2 \quad (3.13)$$

According to (3.11) and (3.12), the self-consistency requirement is satisfied if the propagator functions are independent of k_0 and even functions of \mathbf{k} .

When (3.9) is used for $F(\mathbf{s} - \mathbf{k})$, the gluon functions become

$$F_1(\mathbf{k}) = \lambda\alpha A(\mathbf{k}) + \bar{F}_1(\mathbf{k}) \quad (3.14a)$$

$$F_2(\mathbf{k}) = \lambda\alpha / A(\mathbf{k}) + \bar{F}_2(\mathbf{k}) \quad (3.14b)$$

where the overbar over a function indicates the absence of an infrared singularity. Assumption (2) of the model and (3.14) are mutually consistent since $A(\mathbf{k})$ is infrared finite.⁴

$$\begin{aligned} A(\mathbf{k})^2 &= \frac{1 + F_1(\mathbf{k})}{k^2 + F_2(\mathbf{k})} = \frac{\alpha\lambda A(\mathbf{k}) + 1 + \bar{F}_1(\mathbf{k})}{\frac{\alpha\lambda}{A(\mathbf{k})} + k^2 + \bar{F}_2(\mathbf{k})} \\ &= \frac{1 + \bar{F}_1(\mathbf{k})}{k^2 + \bar{F}_2(\mathbf{k})} \quad (3.15) \end{aligned}$$

The poles of the gluon propagator are located at

$$k_0 = \pm(\alpha\lambda + \{[1 + \bar{F}_1(\mathbf{k})][k^2 + \bar{F}_2(\mathbf{k})]\}^{1/2}) \quad (3.16)$$

As $\lambda \rightarrow \infty$ the poles move to $k_0 = \pm\infty$.

The infrared singularity in each quark function defined by (3.12) can also be isolated:

$$1 + G_1(\mathbf{k}) = \left[1 + \frac{\alpha'\lambda}{2E(\mathbf{k})} \right] [1 + \bar{G}_i(\mathbf{k})] \quad (3.17)$$

where the quark energy is $E(k) = \alpha'\lambda/2 + \bar{E}(k)$ and

$$\bar{E}(\mathbf{k}) = [k^2(1 + \bar{G}_1)^2 + m^2(1 + \bar{G}_2)^2]^{1/2} \quad (3.18)$$

Using (3.17) and (3.18) in the integrals defining G_1 and G_2 , one finds

$$\bar{G}_1(\mathbf{k}) = \frac{\alpha'}{2} \int d^3s \bar{F}(\mathbf{s} - \mathbf{k}) \frac{1 + \bar{G}_1(\mathbf{s})}{\bar{E}(\mathbf{s})} \frac{\mathbf{k} \cdot \mathbf{s}}{k^2} \quad (3.19a)$$

$$\bar{G}_2(\mathbf{k}) = \frac{\alpha'}{2} \int d^3s \bar{F}(\mathbf{s} - \mathbf{k}) \frac{1 + \bar{G}_2(\mathbf{s})}{\bar{E}(\mathbf{s})} \quad (3.19b)$$

Again there is no dependence on the infrared cutoff parameter. The poles of the quark propagator are located at

$$k_0 = \pm \left[\frac{\alpha' \lambda}{2} + \bar{E}(\mathbf{k}) \right]. \quad (3.20)$$

As the cutoff parameter $\mu \rightarrow 0$, the poles move to $k_0 = \pm \infty$.

In order to fully validate the self-consistent model, it is necessary to show that there exist solutions with the expected behavior. The gluon equations must be solved simultaneously for $D(\mathbf{p})$, $F(\mathbf{p})$, and $A(\mathbf{p})$. Then $F(\mathbf{p})$ is used to determine $G_1(\mathbf{p})$ and $G_2(\mathbf{p})$. First, however, ultraviolet divergences must be removed. The renormalization of the pairs (3.1),(3.2) and (3.4),(3.5) is discussed in Ref. 3 and Appendix D. The set of equations in the gluon sector is

$$\frac{1}{g(\mathbf{k})} = -[I(\mathbf{k}) - I(0)], \quad (3.21a)$$

$$F(\mathbf{k}) = \frac{1}{k^2} \frac{g(\mathbf{k})^2}{g(\mathbf{v})^2} \{1 + g(\mathbf{v})^2 [J(\mathbf{k}) - J(\mathbf{v})]\}, \quad (3.21b)$$

$$\begin{aligned} & \frac{1 + \bar{F}_1(\mathbf{k}) - \bar{F}_1(\mathbf{v})}{A(\mathbf{k})^2} - \frac{1 + \bar{F}_1(0) - \bar{F}_1(\mathbf{v})}{A(0)^2} \\ & = k^2 + \bar{F}_2(\mathbf{k}) - \bar{F}_2(0) - \frac{k^2}{v^2} [\bar{F}_2(\mathbf{v}) - \bar{F}_2(0)], \end{aligned} \quad (3.21c)$$

where $gD(\mathbf{k}) = g(\mathbf{k})/k^2$ and all functions and coupling constants are renormalized. Integrals are infrared finite. The limits $g(0) = \infty$ and $A(0) = 1/M$, $M \neq 0$, have been imposed. $A(0)$ is a naturally occurring parameter with dimensions of mass but which is not calculable. It sets the scale of the theory. The linear nature of the integral equation for $F(\mathbf{k})$ is used to set $v^2 F(\mathbf{v}) = 1$. Since v is an arbitrary subtraction point, solutions to (3.21) should not be sensitive to its value. Solutions will not be stable under iteration if the choice of $g(0)$ and $A(0)$ is not consistent with the equations.

One can show analytically that all functions approach their asymptotically-free values in the ultraviolet limit. There are logarithmic modifications to power-law behavior, and the coefficient of the logarithms differs from that predicted by conventional QCD calculations.³ The difference is expected, since the ordering of infrared and ultraviolet limits eliminates diagrams which contribute to standard perturbative QCD calculations. It is important to note, however, that (3.21) is fully renormalized without the missing diagrams.

Analytic solutions to (3.21) are available in the $\mathbf{k} \rightarrow 0$ limit:

$$\lim_{\mathbf{k} \rightarrow 0} g(\mathbf{k}) = \left[\frac{21\pi}{2N} \right]^{1/2} (k/M)^{-1/2}, \quad (3.22a)$$

$$\lim_{\mathbf{k} \rightarrow 0} A(\mathbf{k}) = 1/M, \quad (3.22b)$$

$$\lim_{\mathbf{k} \rightarrow 0} F(\mathbf{k}) = \frac{f}{k^2} \left[\frac{k^2}{M^2} \right]^{-1 \pm i\theta}, \quad (3.22c)$$

where $\theta = 0.0847$ is the solution of

$$\frac{64}{21\pi} = \frac{\sin \pi \theta}{\pi \theta} \frac{1}{(1 + \theta^2) \cosh \pi \theta}, \quad (3.23)$$

and f is not fixed. If $64/21\pi = 0.97 \simeq 1$, $\theta \simeq 0$. The presence of a complex power in (3.27c) is a defect of this lower-order calculation. A linear, nonrelativistic potential in configuration space corresponds to $\theta = 0$ and $F(\mathbf{k}) \propto k^{-4}$. Fortunately θ is small, and there is the expectation that higher-order corrections will produce a purely real power-law dependence for $F(\mathbf{k})$. In the nonrelativistic limit, the Fourier transform of $F(\mathbf{k})$ is the configuration-space potential. Since M is the dimensionful scale factor in the potential, the size of a color-singlet bound state is of order $1/M$. The deviation from a linear potential for this small value of θ does not become significant (i.e., 10%) until $r \simeq 400/M$. Pair production of hadrons becomes important well before that limit. This argument also suggests the nature of important corrections to $F(\mathbf{k})$. Section VI and Appendix E are devoted to a discussion of corrections.

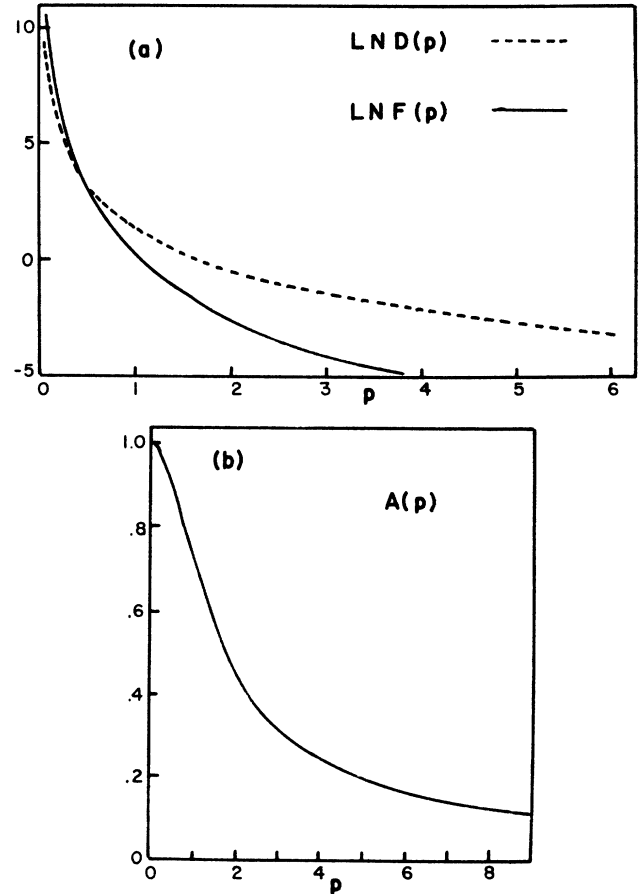


FIG. 3. Numerical solutions of the fundamental equations of the mean-field model are shown as functions of p . The coupling constant in the equation for $F(p)$ is multiplied by 0.9 to avoid complex solutions at $p = 0$. The logarithms of both $D(p)$ and $F(p)$ are plotted in (a), and the gluon propagator function $A(p)$ is given in (b). $F(p)$ is constrained by $F(1) = 1$. The quark counterterm functions $G_1(p)$ and $G_2(p)$ are zero on the scale of (b), except for the highest momenta. The momentum p is measured in units of $A(0)^{-1}$.

Appendix F presents an alternative calculation of $F(\mathbf{k})$. Direct evaluation of the VEV of the integral defining F_{ab} as the product of two Green's-function operators leads to exactly the same singular behavior. One interprets the result as due to the formation of a color-singlet "bound state" of two D -type Coulomb lines interacting by gluon exchange. The alternate derivation is useful for the analysis of possible corrections.

The quark equations are renormalized in Appendix D. The result is

$$1 + \bar{G}_1(k) = 1 + [I\bar{G}_i(k) - I\bar{G}_i(v)] , \quad (3.24)$$

where $I\bar{G}_i(k)$ is the integral on the right-hand side of (3.19). The quark mass and all functions are renormalized.

An approximate numerical solution of the complete set of equations is shown in Fig. 3. Since there exist in lowest-order solutions that satisfy the self-consistency conditions, the next step is to prove confinement and the formation of finite-energy, color-singlet bound states.

IV. WILSON LOOP

The model is designed to confine color and provide a method for calculating the properties of color-singlet bound states. The absence of poles in single particle propagators is one manifestation of confinement. A second way to prove confinement is to calculate the VEV of the Wilson Loop for pure imaginary time τ . A third "proof" requires analysis of the Bethe-Salpeter equation.

The Wilson loop^{8,22} calculation is a nontrivial test of the model. The result depends both on the instantaneous nature of the Coulomb interaction and on the impossibility of propagating physical gluons over finite time intervals. The quantity of interest is

$$L \equiv \left\langle P \left[\exp \left[i \oint A dl \right] \right] \right\rangle , \quad (4.1)$$

where P indicates ordering of field operators around a closed loop. The loop is fixed to be a rectangle with corners $(0,0)$, $(\mathbf{n}R,0)$, $(\mathbf{n}R,T)$, and $(0,T)$. With this choice, L is equal to

$$L = \left\langle \text{tr} \left[P \exp \left[i \int_0^R d\sigma A_n(\mathbf{n}\sigma, 0) \right] P \exp \left[i \int_0^T d\tau A_4(\mathbf{n}R, \tau) \right] P \exp \left[i \int_R^0 d\sigma A_n(\mathbf{n}\sigma, \tau) \right] P \exp \left[i \int_T^0 d\tau A_4(0, \tau) \right] \right] \right\rangle . \quad (4.2)$$

In (4.2) $A_\mu(\mathbf{x}, \tau) = A_\mu^a(\mathbf{x}, \tau)\lambda^a$ and $A_n = \mathbf{n} \cdot \mathbf{A}$. Before (4.2) can be evaluated, it is necessary to define a propagator for the time component of the gluon field. In the Coulomb gauge $A_0^a(\mathbf{x}, t)$ is eliminated from the Hamiltonian. However, the coupling of the time component of the quark current to the modified Coulomb interaction shows how an external source coupled to $A_0^a(\mathbf{x}, t)$ enters the Hamiltonian. The propagator is

$$\langle A_0^a(k) A_0^k(p) \rangle = \frac{i}{(2\pi)^4} \delta_{ab} \delta^4(p+k) g^2 F(\mathbf{k}) . \quad (4.3)$$

To calculate the Wilson loop, one needs propagators in configuration space for imaginary time. Equation (2.10a) with $k_0 \rightarrow ik_4$ is equivalent to

$$\langle A_i^a(x) A_j^b(y) \rangle = \frac{\delta_{ab}}{2(2\pi)^3} \int d^3k P_{ij}(\mathbf{k}) A(\mathbf{k}) e^{-i\mathbf{k} \cdot (\mathbf{x}-\mathbf{y})} e^{-\omega(\mathbf{k}) |x_4 - y_4|} \quad (4.4)$$

and

$$\langle A_4^a(x) A_4^b(y) \rangle = \frac{g^2 \delta_{ab}}{(2\pi)^3} \delta(x_4 - y_4) \int d^3k e^{-i\mathbf{k} \cdot (\mathbf{x}-\mathbf{y})} F(\mathbf{k}) = \delta(x_4 - y_4) \delta_{ab} V(\mathbf{x}-\mathbf{y}) . \quad (4.5)$$

The gluon energy is $\omega(\mathbf{k}) = \alpha\lambda + [(1 + \bar{F}_1)(k^2 + \bar{F}_2)]^{1/2}$. Since the propagator for transverse gluons is proportional to $\exp(-\alpha\lambda |x_4 - y_4|)$, physical gluons do not propagate over finite time intervals. Only when $x_4 = y_4$ is the propagator nonzero in the $\lambda \rightarrow \infty$ limit.

Since the transverse gluons do not propagate over finite time intervals, the spacelike parts of the loop at $\tau = T$ and at $\tau = 0$ are disconnected from each other, and the loop factors into

$$L = G(R)^2 \left\langle P \left[\exp \left[i \int_0^T d\tau A_4(\mathbf{n}R, \tau) \right] P \exp \left[i \int_T^0 A_4(0, \tau) d\tau \right] \right] \right\rangle , \quad (4.6)$$

where

$$G(R) = \frac{1}{N} \left\langle P \text{tr} \left[\exp \left[i \int_0^R d\sigma A_n(\mathbf{n}\sigma, 0) \right] \right] \right\rangle . \quad (4.7)$$

$G(R)$ is τ independent. Term by term $G(R)$ approaches unity as $R \rightarrow \infty$. Confinement comes from the remaining VEV in (4.6). There are contributions from equal τ propagators acting across the loop from $\mathbf{x} = \mathbf{n}R$ to $\mathbf{x} = 0$. In addition it is possible for a τ -like gluon to be emitted and reabsorbed by the same side. Details of the calculation are in Appendix H. The result is

$$L = NG(R)^2 \exp\{-\rho[V(0) - V(R)]T\} . \quad (4.8)$$

If $F(\mathbf{k})$ is given by (3.6) with $n = 2$,

$$\rho V(R) = -\frac{g^2(N^2-1)}{4\pi N} fR, \quad (4.9)$$

and the exponential in the Wilson loop has the standard area dependence. Although $n=2$ seems to be favored by self-consistency, Eq. (4.8) is valid for any value of n . The Wilson loop measures field energy of widely separated sources of color. An area dependence is equivalent to a linear potential.

The success of this calculation depends on the instantaneous propagation of the modified Coulomb interaction. Finite propagation time would lead to crossed rungs and longer-range (in τ) interactions along a side of the loop. If physical gluons propagate over finite time intervals there are additional complications.

V. BOUND STATES

There is a large gap between a general proof of confinement and the derivation of explicit bound-state equations. The self-consistent model incorporates the full machinery of field theory. Thus, it is possible to derive Bethe-Salpeter equations for both gluon-gluon and quark-quark states. Although the three-quark calculation is possible,²³ it is not discussed here.

The derivation of the Bethe-Salpeter equation for quarks is straightforward. One considers ladder diagrams for quark-antiquark scattering. The color-singlet channel is projected out. Summation of the ladder diagram leads to an inhomogeneous integral equation. The homogeneous version for bound states is

$$\Psi_{\alpha\beta}(\mathbf{p}, \mathbf{W}; W_0) = \frac{i\alpha'}{(2\pi)} \int d^4x F(\mathbf{p}-\mathbf{x}) [\gamma_0 S(-W/2-x)]_{\alpha\alpha'} \Psi_{\alpha'\beta'}(\mathbf{x}, \mathbf{W}; W_0) [S(W/2-x)\gamma_0]_{\beta\beta'}. \quad (5.1)$$

The x_0 integration introduces the standard positive- and negative-energy projection operators:

$$\Lambda_{\pm}(\mathbf{k}) = \frac{1}{2} \left[1 \pm \frac{\gamma_0 \boldsymbol{\gamma} \cdot \mathbf{k} [1 + \bar{G}_1(k)] + \gamma_0 m [1 + \bar{G}_2(k)]}{\bar{E}(k)} \right]. \quad (5.2)$$

The quark Bethe-Salpeter equation is

$$\Psi(\mathbf{p}, \mathbf{W}; W_0) = \alpha' \int d^3x F(\mathbf{p}-\mathbf{x}) \left[\frac{\Lambda_-(\mathbf{W}/2-\mathbf{x})\Psi(\mathbf{x}, \mathbf{W}; W_0)\Lambda_+(-\mathbf{W}/2+\mathbf{x})}{\Sigma_f + W_0} + \frac{\Lambda_+(-\mathbf{W}/2-\mathbf{x})\Psi(\mathbf{x}, \mathbf{W}; W_0)\Lambda_-(-\mathbf{W}/2+\mathbf{x})}{\Sigma_f - W_0} \right] \quad (5.3)$$

and $\Sigma_f = E(\mathbf{W}/2+\mathbf{x}) + E(\mathbf{W}/2-\mathbf{x}) = \alpha'\lambda + \bar{\Sigma}_f$. The projection operators are independent of $\lambda(\mu)$. Since the interaction is instantaneous, the Bethe-Salpeter equation becomes the Breit equation.

A finite equation is possible only if there is a cancellation between λ in Σ_f and $F(\mathbf{p}-\mathbf{x}) \propto \lambda \delta^3(\mathbf{p}-\mathbf{x})$. In all qq and $\bar{q}q$ channels, except the color-singlet one, infrared cancellation requires $\Psi \equiv 0$. The color-singlet wave function becomes $\Psi = \Psi_{+-} + \Psi_{-+}$, where the subscripts indicate left and right projection with Λ_+ or Λ_- . In other words, $\Lambda_+ \psi \Lambda_+ = \Lambda_- \psi \Lambda_- = 0$. It is convenient to define new amplitudes by

$$\Psi_{\pm\mp} = (\Sigma_f \pm W_0) \Phi_{\pm\mp}, \quad (5.4)$$

in order to remove divergent factors from the denominator of (5.3). The bound-state equations are

$$[\bar{\Sigma}_f(\mathbf{p}, \mathbf{W}) - W_0] \Phi_{-+}(\mathbf{p}, \mathbf{W}, W_0) = \Lambda_-(-\mathbf{W}/2-\mathbf{p}) \times \left[\alpha' \int d^3x \bar{F}(\mathbf{p}-\mathbf{x}) [\Phi_{-+}(\mathbf{x}, \mathbf{W}; W_0) + \Phi_{+-}(\mathbf{x}, \mathbf{W}; W_0)] \right] \Lambda_+(\mathbf{W}/2-\mathbf{p}), \quad (5.5a)$$

$$[\bar{\Sigma}_f(\mathbf{p}, \mathbf{W}) + W_0] \Phi_{+-}(\mathbf{p}, \mathbf{W}, W_0) = \Lambda_+(-\mathbf{W}/2-\mathbf{p}) \times \left[\alpha' \int d^3x \bar{F}(\mathbf{p}-\mathbf{x}) [\Phi_{-+}(\mathbf{x}, \mathbf{W}; W_0) + \Phi_{+-}(\mathbf{x}, \mathbf{W}; W_0)] \right] \Lambda_-(\mathbf{W}/2-\mathbf{p}). \quad (5.5b)$$

In the center-of-momentum frame where $\mathbf{W}=0$, these equations are identical to the Tamm-Dancoff equations of Ref. 2. There it was shown, both numerically and with the WKB approximation, that there exists an infinite number of bound states. The Bethe-Salpeter equation, unlike the Tamm-Dancoff²⁴ equation, can be renormalized.

The phenomenology of bound states is beyond the scope of this paper. However, one can easily show that in

the nonrelativistic limit of heavy quarks, the Bethe-Salpeter equation reduces to the Schrödinger equation with a confining potential proportional to $r^{n-3/2}$. Leading corrections to the nonrelativistic limit introduce $\mathbf{L} \cdot \mathbf{S}$ coupling, but spin-spin and tensor interactions are not found. The equations are defined for nonzero total momentum, i.e., bound states in motion. Another property of these equations is that they are defined even when the quarks have zero bare mass. When the quark propa-

gator function is redefined by setting $1+G_2(p) = G_2'(p)/m$ in (2.9), the nonlinear equations for $G_1(p)$ and $G_2'(p)$ are well defined. Having done this, one can project the 0^{+-} channel out of (5.4) and look for $W_0=0$ solutions. If the pion wave function is identified with $G_2'(p)$, the bound-state equation is identical to the consistency equation for $G_2'(p)$. The model predicts the existence of a zero-mass pion.²⁵ Chiral symmetry is broken and one can study the formation of a $q\bar{q}$ condensate.

The analysis of bound states in the gluon sector is complicated by the spin of the gluon and the need to consider the three different gluon propagators of (2.10). Ladder diagrams with Coulomb exchange lead to a set of coupled integral equations for color-singlet glueballs. The equations are identical to those of Ref. 3 with a change in kinematics for fully dressed gluons.

Corrections to the set of ladder diagrams are calculable. Most vanish in the $\lambda(\mu) \rightarrow \infty$ limit. There is no glueball-meson mixing. A more interesting extension examines the effects of finite-energy bound-state poles in two-particle Green's functions. Since Bethe-Salpeter wave functions can be normalized by standard methods, it is possible to project out hadronic contributions to quark scattering processes.²⁶

VI. CORRECTIONS

The self-consistent model describes a world in which single quarks and gluons have infinite energy, yet color-singlet bound states with finite energy exist. The model should provide a useful theoretical laboratory for the study of the relationship between bound state and constituent degrees of freedom. Since the full machinery of QCD is available, albeit in a particular gauge, one can analyze a number of corrections. This is a useful exercise in order to understand whether this model might be an accurate description of the confinement process in QCD. Here I consider questions that are answerable within the framework of the model. Perturbation theory with effective propagators is used to investigate the stability of the results of Sec. III. I address in turn the effect of anomalous interactions, vertex corrections, screening, ordering of the $\mathbf{p} \rightarrow 0$ and $\mathbf{p} \rightarrow \infty$ limits, and finite higher-order corrections.

A. Anomalous interactions

The $V_1(A)$ and $V_2(A)$ terms in the Coulomb-gauge Hamiltonian have been ignored in the development of a low-momentum theory. These interactions are required for correct quantization^{10,14} and have been shown to be necessary for renormalizability.²⁷ They cancel divergences of order g^4 and higher and allow one to reproduce standard calculations of gauge-invariant quantities. Neglect of $V_1(A)$ and $V_2(A)$ is equivalent to the state-

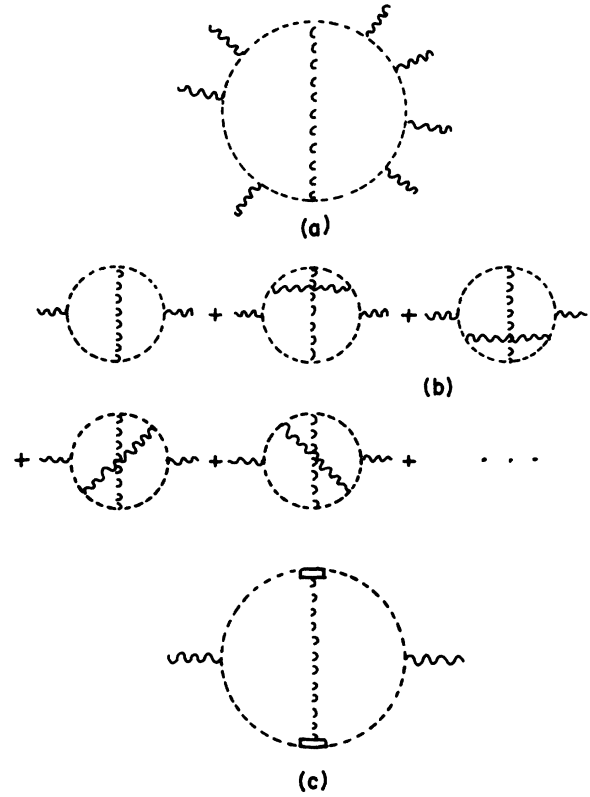


FIG. 4. A representative multigluon interaction arising from $V_1(A)$ is shown in (a); vertices are taken to be points. The dashed-wavy line represents a fictitious gluon line. Order- g^4 and $-g^6$ corrections to the gluon self-energy appear in (b). A large class of planar diagrams sum in (c) to produce vertex corrections for the fictitious gluon.

ment that they have no qualitative effect in the infrared limit. Since neither quark fields nor momentum fields $P_i^a(p)$ are directly affected by anomalous interactions, the only way they can scuttle the self-consistent model is for them to generate two- and/or four-gluon interactions which are infrared singular. A definite statement requires a reliable nonperturbative calculation. Such a calculation is difficult even with the simplified perturbation theory.

The structure of $V_1(A)$, as shown in Fig. 4(a), is that of a closed loop of D -type Coulomb propagators bisected by a fictitious gluon line that carries momentum, color, and spin, but does not have a propagator. An effective two-gluon coupling is derived from the operator-product expansion of each $D_{ab}(\mathbf{p}, \mathbf{k}; x)$ in (A2). [See Fig. 4(b).] Gluons in the expansion couple either to external particles or to the opposing Coulomb line. Keeping just planar diagrams, one can sum the terms of Fig. 4(b) to give Fig. 4(c). If all vertices are replaced by points, the effective two-gluon action due to $V_1(A)$ is

$$\int dt V_1(A) = -\frac{g^4 N^2}{16(2\pi)^2} \int d^4 p d^4 k \delta^4(p+k) A_i^a(p) A_j^a(k) \times \left[\int d^3 s s_i(p-s)_m D(s) D(\mathbf{p}-s) \int d^3 t t_j(k-t)_m D(t) D(\mathbf{k}-t) \right]. \quad (6.1)$$

This expression is to be compared with the $A_i^a(p)A_i^a(k)$ term in (2.9). The s and t integrals in (6.1) are infrared convergent but ultraviolet divergent in order to cancel g^4 divergences in the standard Coulomb Hamiltonian and $V_2(A)$. If the s and t integrals are cut off at infinity and evaluated with $D(s) \propto M^{1/2}S^{-5/2}$ and $A(0)=1/M$, the factor in large parentheses is proportional to M^2 . Compare this result with the propagator function $F_2(\mathbf{k})$ which has a divergence proportional to $\lambda(\mu)$ and a finite term proportional to $1/k$ for a linear confining interaction.

Although (6.1) does not have an infrared singularity, there is the possibility that a singularity could develop from nonperturbative effects at the vertices in Fig. 4(c). However, vertex corrections do not alter infrared behavior. The conclusion is that when $V_1(A)$ is treated like the Coulomb interaction, it does not produce an infrared singularity.

The three terms in $\int V_2(A)$ are analyzed in the same way. Again there are real and fictitious gluon lines. The modified Coulomb interaction appears explicitly. The apparent singularity from $F(p)$ is suppressed by gluon-projection operators. Wherever it appears, $F(p)$ is replaced by the nonsingular function $\bar{F}(p)$. Figure 5 summarizes the contributions of $V_2(A)$ to the two-gluon action in the point vertex limit. There is a singular term of the form

$$\int V_2(A)dt = -\frac{g^2 N^2}{8(2\pi)^2} \int d^4p d^4k \delta^4(p+k) A_i^a(p) A_j^a(k) \times \int d^3s d^3t \left[s_i s_j \text{tr}[P(\mathbf{s})P(\mathbf{s}-\mathbf{t})] \frac{d}{dg} [g^3 D(\mathbf{s})D(\mathbf{s})D(\mathbf{s}+\mathbf{p})] + \dots \right], \quad (6.2)$$

where $d[gD(p)]/dg = F(p)$. Note that the infrared-divergent s integral is multiplied by an ultraviolet-divergent t integral. This term must cancel a higher-order term in the standard Coulomb Hamiltonian. Other

integrals in $\int V_2(A)$ match the $1/k$ divergence in the propagator function $F_2(k)$. Together with contributions from the Coulomb interaction, these terms produce a renormalizable correction to the calculation of the gluon propagator function $A(p)$. Thus, in the infrared limit, the only effect of the anomalous interactions is to produce small corrections to the fundamental equations. They do not generate a qualitatively different momentum dependence or alter the nature of the singularity.

B. Vertex corrections

All calculations in this model are done in the limit of point coupling of gluons to Coulomb lines. Appendix E contains a discussion of vertex corrections due to a finite number of gluon lines connecting across the external gluon. Examples are shown in Figs. 6(a) and 6(b). The general conclusion of power-counting arguments is that vertex integrals are convergent. No renormalization is necessary. More importantly, there are no infrared singularities. A point vertex is proportional to p , and vertex corrections are proportional to p in the infrared limit. Replacement of vertex functions by point vertices has no qualitative effect. A numerical calculation of Fig. 6(c) in the infrared limit finds a 5% shift in the coefficient of $p^{-5/2}$ in $D(p)$.

A more general vertex correction is produced when the two Coulomb lines on either side of the gluon interact to form a bound state. As shown in Appendix F, the singular function $F(p)$ is the color-singlet bound state of two D -type Coulomb lines when the total momentum is zero. However, this infrared singularity is unlikely to affect vertex functions. Color-singlet binding across a vertex is suppressed in the $N \rightarrow \infty$ limit of $SU(N)$. In addition the total momentum zero region is an infinitesimal part of the integration volume sampled by a vertex integral.

The conclusion is that the part of vertex functions that couple to *transverse* gluons does not affect the infrared limit. The longitudinal part of the vertex is decoupled from the theory.

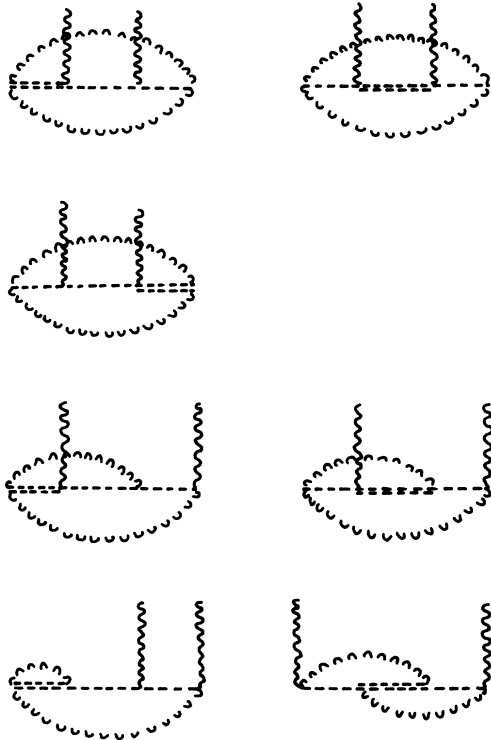


FIG. 5. The anomalous interaction $V_2(A)$ produces seven diagrams which contribute to the gluon self-energy. All have two fictitious gluons (dashed-wavy line), two $D(p)$ propagators (dashed line), and a single $F(p)$ (double-dashed line). Vertex effects are suppressed. The first three are produced by the first term in (A3); the second three come from the second term in (A3). The final diagram arises from the third term.

C. Screening

The existence of an infrared singular modified Coulomb interaction is very important to the success of the self-consistent model. It is possible that the singularity in $F(p)$ is eliminated by the screening effects of quark and gluon pairs. When one includes quark and gluon loop insertions in the singular Coulomb propagator, the function $F(p)$ is replaced by $F'(p)$ in the Bethe-Salpeter equations of Sec. V and inside the integrals of (3.21). The two functions are related by

$$F'(k)^{-1} = F(k)^{-1} + I_G(k) + I_Q(k). \quad (6.3)$$

The gluon loop integral is

$$I_G(k) = -\frac{\alpha}{2} \int d^3s d^3t \delta^3(s+t-k) \text{tr}[P(s)P(t)] \\ \times \left[\frac{A(s)}{A(t)} + \frac{A(t)}{A(s)} - 2 \right] \\ \times \frac{2\alpha\lambda + \bar{\omega}(s) + \bar{\omega}(t)}{[2\alpha\lambda + \bar{\omega}(s) + \bar{\omega}(t)]^2 - k_0^2} \quad (6.4)$$

and the quark $I_Q(k)$ has a similar form. Both integrals are logarithmically divergent, functions of k_0^2 as well as \mathbf{k}^2 , and of order λ^{-1} . They are also proportional to k^2 in the $k \rightarrow 0$ limit. If $\lambda \rightarrow \infty$, both integrals vanish. Closer analysis reveals a problem. If one considers the dependence on the cutoff parameter μ , one discovers that I_G and I_Q are proportional to $\mu^{2n-3}k^2$. Therefore, if $F(k)^{-1} \propto (k^2 + \mu^2)^n$,

$$F'(k)^{-1} = (k^2 + \mu^2)^n + \beta\mu^{2n-3}k^2. \quad (6.5)$$

Integrals with $F(k)$ replaced by $F'(k)$ diverge as $\mu \rightarrow 0$, but the actual μ dependence is not consistent with $\lambda \propto \mu^{3-2n}$. In other words, if (6.5) is true, the infrared singularity in $F(k)$ is not maintained in higher order.

When (6.3) is renormalized, the problem goes away. The quark and gluon integrals are both proportional to k^2 . If $F(k) = f(k)/k^2$, $F'(k) = f'(k)/k^2$, and $I_G(k) + I_Q(k) = k^2 I(k)$,

$$f'(k)^{-1} - f'(v)^{-1} = f(k)^{-1} - f(v)^{-1} + I(k) - I(v). \quad (6.6)$$

The subtraction renders the integrals ultraviolet finite. Choosing $v=0$ and requiring $f'(0)^{-1} = f(0)^{-1} = 0$, one finds

$$f'(k)^{-1} = f(k)^{-1} + I(k) - I(0). \quad (6.7)$$

Since $I(k) - I(0)$ is proportional to k^2 as $k \rightarrow 0$, the infrared singularity in $f(k)$ is maintained in $f'(k)$. One can safely let $\mu \rightarrow 0$, $\lambda \rightarrow \infty$, and $[I(k) - I(0)] \rightarrow 0$. While it might seem that an obvious point has been belabored, the existence of the infrared singularity in $F'(k)$ as well as in $F(k)$ is absolutely crucial for the whole model. Screening does not remove the singularity.

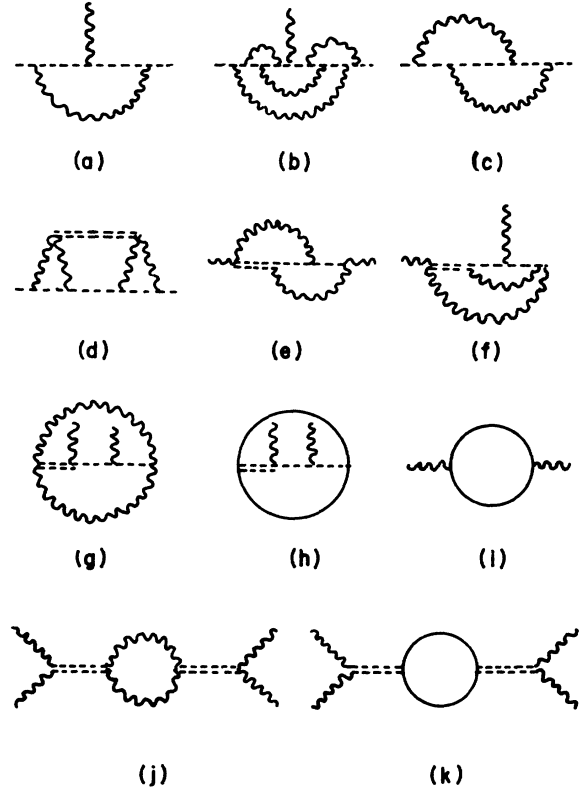


FIG. 6. The first correction to a point vertex on a D -type Coulomb line is shown in (a), while (b) suggests the complexity of higher-order vertices. Substitution of (a) into the equation for $D(p)$ requires evaluation of (c). A second correction to $D(k)$ is produced by (d). The double-dashed line is an $F(p)$ propagator. Diagrams (e)–(h) are the g^4 corrections to the gluon self-energy associated with the two-gluon term in the operator expansion of $F_{ab}(\mathbf{p}, \mathbf{k}; x)$. Each diagram shows one of three positions for the singular Coulomb line. Diagram (i) is the quark-loop term in the gluon propagator, and (j) and (k) show gluon and quark-loop corrections to the Coulomb interaction between gluons.

D. Limit ordering

The gluon effective propagator is not affected by the insertion of the quark loop in Fig. 6(i). The rules for counting powers of λ suggest that the quark loop should be of order λ^{-1} . On the other hand, the loop integral is quadratically divergent. Using dimensional regularization, one finds that the coefficient of the pole at $d=3$ dimensions is proportional to λ^2 . In addition the quark loop is an explicit function of k_0 . The renormalization prescription used in Appendix D involves subtractions at $\mathbf{k}^2=0$ and $\mathbf{k}^2=v^2$. After subtraction, the residual finite integral vanishes as $\lambda \rightarrow 0$. The prescription for handling the infrared limit is valid even when renormalization is performed before setting $\mu=0$.

E. Finite higher-order corrections

The renormalized integral equation for $F(p)$ represents a one-loop calculation. Self-consistency in the infrared

limit was only approximate due to the appearance of a complex power law. Higher-order corrections in the equation for $F(p)$ are generated by using $F(p) = d[gD(p)]/dg$ on the corrections to the equation for $D(p)$. Figures 6(c) and 6(d) show possible corrections. Power counting in λ shows that Fig. 6(d) is of order λ^{-1} . [The antisymmetric coupling of $F(p)$ to A_1^a and P_i^a suppresses the singularity in $F(p)$ when gluon type is summed over.] There are three $D(k)$ propagators in Fig. 6(c), and differentiation generates three diagrams. Two of them are equivalent to replacing the point vertex in the lowest-order calculation by a dressed vertex. In the third diagram, the central Coulomb propagator in Fig. 6(c) becomes singular. [When $F(p)$ is thought of as the zero-energy bound state of two D -type lines, this diagram is the crossed box correction to the kernel of the ladder approximation Bethe-Salpeter equation.] Numerical evaluation of just this diagram together with the correction to $D(k)$ produces a 2% shift towards eliminating the complex power law in the Coulomb interaction. If vertex corrections are partially included, the shift is away from a real power law. What is needed is a simultaneous solution of Dyson equations for vertex functions and propagator functions.

Corrections to the gluon propagator functions are of interest. The full set of nonvanishing order- g^4 diagrams is displayed in Figs. 6(e)–6(h). As shown in Appendix E, there are no infrared divergences. Integrals are finite in the $\lambda \rightarrow \infty$ limit. These diagrams produce small corrections in the propagator functions but do not affect the infrared divergence that removes gluons from the physical spectrum.

VII. DISCUSSION

This paper presents a model of the confinement process in QCD. In a domain where conventional perturbation theory is useless, progress is possible only if assumptions are made about the physics of the infrared limit. The results are believable only if the assumptions are shown to be consistent with the fundamental theory and if they lead to a reasonable picture of the world. Consistency with QCD is self-consistently verified by direct calculation coupled with stability against corrections. The reasonable world picture is built in by the nature of the assumptions.

Are there problems with the model that are sufficiently serious to render it useless as a theoretical laboratory? The choice of gauge constitutes an “in principle” objection that is addressed at length in the introduction. Arguments are presented that the Coulomb gauge, or a gauge much like it, is necessary for any detailed discussion of confinement. Ward identities are a test of the gauge nature of the underlying theory. Appendix G presents a naive Ward identity calculation in the quark sector. Infrared singularities match in the $N \rightarrow \infty$ limit. However, there are too many unanswered questions about the derivation to take the result seriously.

In this model the confining interaction is instantaneous

and transforms as the fourth component of a four-vector. Conventional relativistic bound-state calculations show that the dominant part of the potential can be legitimately treated as instantaneous.²⁸ Phenomenology in the charmed- and bottom-quark sectors favors a long-range interaction that has the structure of a Lorentz scalar.²⁹ That conclusion is based on lowest-order relativistic corrections to the simplest potential model. There are corrections to the interaction in the self-consistent model which are not instantaneous and which have a different Lorentz structure. Bound-state exchange is one example.

There is the annoying problem that in lowest order the infrared limit of $F(k) \propto k^{-2n}$ is almost, but not quite, consistent with the favored value $n=2$. The fact that $n=2 \pm i\epsilon$ is of concern. Many possible corrections vanish in the infrared limit. On the other hand, the power dependence of $F(k)$ is fixed in a way that makes it sensitive to corrections. The behaviors of the Green's function $D(k)$ and the propagator function $A(k)$ are fixed by matching powers of momenta in the consistency equations. $F(k)$ is subject to the more demanding requirement that the coefficients of the power must match. Higher-order corrections do not change the power dependence of $D(k)$ and $A(k)$ but do affect $F(k)$.

The ordering of infrared and ultraviolet limits is a delicate point. When the infrared limit is taken first, the three-gluon, four-gluon, and quark-quark-gluon vertices are eliminated from the theory. All that remains are couplings to Coulomb lines. Reversing the order would restore the correct asymptotic freedom limit without significantly altering the low-momentum structure, but the cost would be a large increase in complexity. As it stands, perturbation theory is still complicated by the need to treat nonlocal interactions of indefinite order in the coupling constant. Strict perturbation theory to order g^n requires order- g^n terms from the Coulomb Hamiltonian (and anomalous interactions) as well as g^n contributions from higher powers of the Hamiltonian. The operator-product expansion helps, but one needs a method to identify the most important infrared finite amplitudes. As a general rule calculations in the quark sector are simpler than in the gluon sector. There is only one type of quark-quark-Coulomb coupling. Gluons couple to Coulomb lines in pairs at the end, singly in the middle, and through anomalous interactions.

The technical problems of the self-consistent model should not detract from its usefulness as a theoretical laboratory for the study of bound states. The spectrum and wave functions in the nonrelativistic limit² are similar to those found in *ad hoc* treatments of heavy-quark physics.³⁰ The advantage here is that there is a clear identification of possible corrections to lowest-order calculations. When weak-electromagnetic interactions are included, the calculation of static matrix elements is conceptually straightforward. Extension to bound states of three quarks is possible. The presence of a zero-mass pion in the limit of massless quarks opens the area of chiral-symmetry breaking.²⁵ Purely hadronic processes are calculable in principle. Wave functions for bound states in motion are required. The Bethe-Salpeter equations of Sec. V provide a framework for calculating such

wave functions. The two-quark Green's function contains a set of bound-state poles with calculable residues. A purely hadronic process such as pion-pion elastic scattering can be extracted from the $q\bar{q}q\bar{q} \rightarrow q\bar{q}q\bar{q}$ scattering amplitude. The meaning of a scattering amplitude for infinite-energy particles is not obvious. Although internal quark lines are suppressed, there are enough problems

with hadronic intermediate states to make such calculations impractical.

ACKNOWLEDGMENT

This research was supported in part by a grant from the National Science Foundation.

APPENDIX A: ANOMALOUS INTERACTIONS

In configuration space $V_1(A)$ is given by¹⁰

$$V_1(A) = -\frac{g^2}{8} \int d^3r d^3r' d^3r'' f_{ade} f_{bec} [D_{ab}(\mathbf{r}, \mathbf{r}'; t) \nabla_j' \delta^3(\mathbf{r}' - \mathbf{r})] [D_{cd}(\mathbf{r}, \mathbf{r}''; t) \nabla_j'' \delta^3(\mathbf{r}'' - \mathbf{r})]. \quad (\text{A1})$$

In momentum space this becomes

$$\int dt V_1(A) = (2\pi)^4 \frac{g^2}{8} \int d\mathbf{p}_1 d\mathbf{p}_2 d\mathbf{k}_1 d\mathbf{k}_2 dx_1 dx_2 \delta^3(\mathbf{p}_1 + \mathbf{p}_2 + \mathbf{k}_1 + \mathbf{k}_2) \delta(x_1 + x_2) \\ \times f_{ade} f_{cbe} \mathbf{k}_1 \cdot \mathbf{k}_2 D_{ab}(\mathbf{p}_1, \mathbf{k}_1; x_1) D_{cd}(\mathbf{p}_2, \mathbf{k}_2; x_2). \quad (\text{A2})$$

Although $\int dt V_1(A)$ appears to be of order g^2 , the first nonvanishing term is of order g^4 . If either factor of the modified Green's function $D_{ab}(\mathbf{p}, \mathbf{k}; x)$ is replaced by its zero-order value $\delta_{ab} \delta(\mathbf{p} + \mathbf{k}) / p^2$, $\int V_1(A)$ vanishes. The configuration-space form of $V_2(A)$ is complicated. In momentum space the expression is marginally simpler:

$$\int dt V_2(A) = -2\pi \frac{g^2 N}{8} \int d^3p d^3k F_{aa}(\mathbf{p}, -\mathbf{p}; 0) \text{tr}[P(\mathbf{p})P(\mathbf{p} - \mathbf{k})] \\ - 2i(2\pi)^4 \frac{g^3}{8} \int d^3p d^3k d^3s d^3t d^4r dx_1 dx_2 \delta(x_1 + x_2 + r_0) \delta^3(\mathbf{p} + \mathbf{k} + \mathbf{r} + \mathbf{s} + \mathbf{t}) f_{xey} f_{x'fb} f_{y'ac} \\ \times D_{ab}(\mathbf{s}, \mathbf{t}; x_1) F_{ef}(\mathbf{p}, \mathbf{k}; x_2) \mathbf{A}^c(\mathbf{r}) \cdot \mathbf{P}(\mathbf{s} + \mathbf{r}) \cdot \mathbf{P}(\mathbf{t} + \mathbf{k}) \cdot \mathbf{t} \\ + \frac{(2\pi)^7 g^4}{8} \int d^3p d^3k d^3s d^3t d^3s' d^3t' d^4r d^4r' dx_1 dx_2 dx_3 \\ \times \delta^3(\mathbf{p} + \mathbf{t} + \mathbf{r}' + \mathbf{s}') \delta^3(\mathbf{k} + \mathbf{t}' + \mathbf{s} + \mathbf{r}) \delta(x_1 + x_2 + x_3 + r_0 + r_0') \\ \times f_{bex} f_{fb'y} f_{yac} f_{xa'c'} F_{ef}(\mathbf{p}, \mathbf{k}; x_3) D_{ab}(\mathbf{s}, \mathbf{t}; x_1) D_{a'b'}(\mathbf{s}', \mathbf{t}'; x_2) \\ \times [\mathbf{A}^c(\mathbf{r}) \cdot \mathbf{P}(\mathbf{s} + \mathbf{r}) \cdot \mathbf{t}'] [\mathbf{A}^{c'}(\mathbf{r}') \cdot \mathbf{P}(\mathbf{s}' + \mathbf{r}') \cdot \mathbf{t}], \quad (\text{A3})$$

where $P_{ij}(\mathbf{p}) = \delta_{ij} - p_i p_j / p^2$. The first term is manifestly ultraviolet divergent. Contributions from $V_2(A)$ are needed to cancel ultraviolet divergences that arise from the Coulomb interaction.²⁷

APPENDIX B: COULOMB OPERATOR-PRODUCT EXPANSION

When the integral equation for $D_{ab}(\mathbf{p}, \mathbf{k}; x)$ is iterated, the result is an infinite-series expansion in powers of the coupling constant g . Substitution of this series into (2.16), the definition of $F_{ab}(\mathbf{p}, \mathbf{k}; x)$, leads to the relation $F = d[\mathbf{g}D]/d\mathbf{g}$. The structure of the Coulomb interaction operator $F_{ab}(\mathbf{p}, \mathbf{k}; x)$ can be calculated from that of the Green's function operator. The infinite series for $D_{ab}(\mathbf{p}, \mathbf{k}; x)$ is

$$\begin{aligned}
D_{ab}(\mathbf{p}, \mathbf{k}; x) = & \frac{1}{(2\pi)^3} \left[\frac{\delta_{ab} \delta(\mathbf{p} + \mathbf{k}) \delta(x)}{\mathbf{p}^2} + igf_{acb} \frac{1}{\mathbf{p}^2} \mathbf{A}^c(\mathbf{p} + \mathbf{k}, x) \cdot \mathbf{p} \frac{1}{\mathbf{k}^2} \right. \\
& + \sum_{n=2}^{\infty} (ig)^n f_{ac_1 e_1} f_{e_1 c_2 e_2} \cdots f_{e_{n-1} c_n b} \\
& \times \int \frac{d^4 s_1 \cdots d^4 s_n}{\mathbf{p}^2 (\mathbf{p} - \mathbf{s}_1)^2 \cdots \left[\mathbf{p} - \sum_1^n \mathbf{s}_i \right]^2} \delta^3 \left[\mathbf{p} + \mathbf{k} - \sum_1^n \mathbf{s}_i \right] \delta \left[x - \sum s_{i0} \right] \\
& \left. \times \mathbf{A}^{c_1}(s_1) \cdot \mathbf{p} \mathbf{A}^{c_2}(s_2) \cdot (\mathbf{p} - \mathbf{s}_1) \cdots \mathbf{A}^{c_n}(s_n) \cdot \left[\mathbf{p} - \sum_1^{n-1} \mathbf{s}_i \right] \right]. \quad (\text{B1})
\end{aligned}$$

The n th term in this series is comprised of $n+1$ zeroth-order Coulomb propagators, $1/\mathbf{p}^2$, separated by n vertices at which gluon fields are coupled. Momentum is conserved at each vertex. If $D_{ab}(\mathbf{p}, \mathbf{k}; x)$ is a subunit in a Feynman diagram, some of the gluon fields attach to other elements of the diagram, and the rest become gluons that are emitted and reabsorbed by the Coulomb line itself. (See Fig. 1.) An alternative expansion of $D_{ab}(\mathbf{p}, \mathbf{k}; x)$ is

$$\begin{aligned}
D_{ab}(\mathbf{p}, \mathbf{k}; x) = & \langle D_{ab}(\mathbf{p}, \mathbf{k}; x) \rangle + \int d^4 s D_{abc; i}^{(1)}(\mathbf{p}, \mathbf{k}; x; s) A_i^c(s) \delta^3(\mathbf{p} + \mathbf{k} - \mathbf{s}) \delta(x - s_0) \\
& + \sum_{n=2}^{\infty} \int d^4 s_1 \cdots d^4 s_n D_{ac_1 \cdots c_n b; i_1 \cdots i_n}^{(n)}(\mathbf{p}, \mathbf{k}; x; s_1, \dots, s_n) \\
& \times A_{i_1}^{c_1}(s_1) \cdots A_{i_n}^{c_n}(s_n) \delta^3 \left[\mathbf{p} + \mathbf{k} - \sum \mathbf{s}_i \right] \delta \left[x - \sum s_{i0} \right], \quad (\text{B2})
\end{aligned}$$

where the $::$ notation indicates that the gluon fields are to connect to external (i.e., not the same Coulomb line) vertices. Thus, for $n=2$, the contraction between the two field operators is zero. Equation (B2) constitutes an operator-product expansion for $D_{ab}(\mathbf{p}, \mathbf{k}; x)$.

The first term in (B2) is the VEV of the modified Coulomb Green's function. One can either calculate it in perturbation theory or use invariance arguments to show that

$$\langle D_{ab}(\mathbf{p}, \mathbf{k}; x) \rangle = \frac{\delta_{ab}}{(2\pi)^3} \delta(\mathbf{p} + \mathbf{k}) \delta(x) D(\mathbf{p}). \quad (\text{B3})$$

The one-gluon function $D_{abc; i}^{(1)}(\mathbf{p}, \mathbf{k}; x; s)$ has the structure of Fig. 7(a). There are two factors of the VEV of D_{ab} , and the gluon is emitted from a vertex function which in lowest order is proportional to igp_i :

$$D_{abc; i}^{(1)}(\mathbf{p}, \mathbf{k}; x) = \frac{1}{(2\pi)^3} D(p) \{ igf_{acb} [p_i + \Gamma_i(p, k)] \} D(k). \quad (\text{B4})$$

The vertex function $\Gamma_i(\mathbf{p}, \mathbf{k})$ is one-line irreducible. There exists an integral equation for irreducible vertex functions (see Appendix E). The two-gluon function [Fig. 7(b)] is more complicated, but generalization to n gluons is straightforward, at least in principle.

The utility of the operator expansion is that the one-, two-, etc., gluon vertex functions are benign. They are ultraviolet finite and do not change the nature of the infrared singularity. In Appendix E it is shown that each vertex represents a finite, calculable correction to a

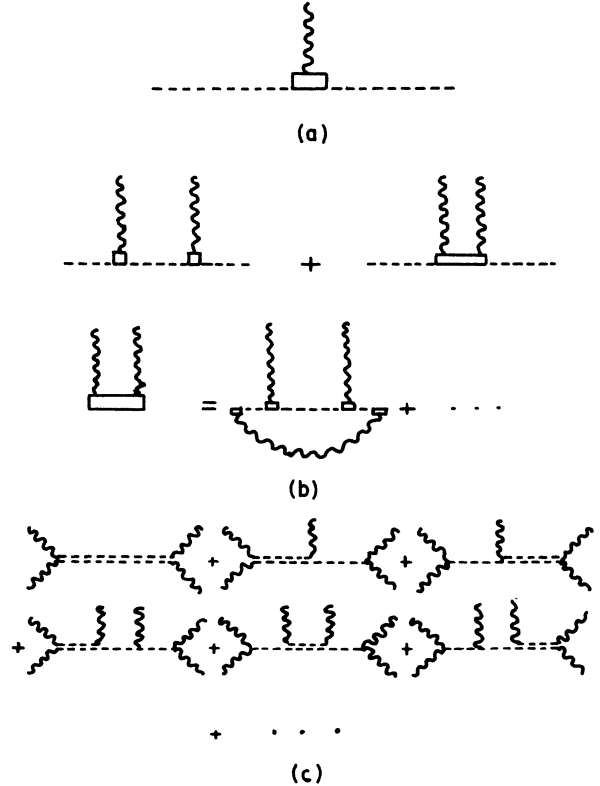


FIG. 7. The one-gluon term in the operator-product expansion of $D_{ab}(\mathbf{p}, \mathbf{k}; x)$ is given in (a) and the two-gluon term in (b). In the absence of vertex corrections, $F_{ab}(\mathbf{p}, \mathbf{k}; x)$ has the operator expansion in (c).

lowest-order result.

If the vertex functions for gluon emission along a Coulomb line are replaced by the momentum factor of lowest-order perturbation theory, the operator expansion of the modified Green's function has exactly the structure of (B1) with each $1/p^2$ replaced by $D(\mathbf{p})$. Gluons couple to external vertices, not to other gluons along the line.

$$\begin{aligned}
F_{ab}(\mathbf{p}, \mathbf{k}; x) = & \frac{1}{(2\pi)^3} \left\{ \delta_{ab} \delta(\mathbf{p} + \mathbf{k}) \delta(x) F(\mathbf{p}) + ig f_{acb} [F(\mathbf{p}) D(\mathbf{k}) + D(\mathbf{p}) F(\mathbf{k})] \mathbf{A}^c(\mathbf{p} + \mathbf{k}; x) \cdot \mathbf{p} \right. \\
& + (ig)^2 f_{ac_1 e_1} f_{e_1 c_2 b} \int d^4 s [F(\mathbf{p}) D(\mathbf{p} - \mathbf{s}) D(\mathbf{k}) + D(\mathbf{p}) F(\mathbf{p} - \mathbf{s}) D(\mathbf{k}) \\
& \quad \left. + D(\mathbf{p}) D(\mathbf{p} - \mathbf{s}) F(\mathbf{k})] : \mathbf{A}^{e_1}(s) \cdot \mathbf{p} \mathbf{A}^{e_2}(\mathbf{p} + \mathbf{k} - \mathbf{s}; x - s_0) \cdot (\mathbf{p} - \mathbf{s}) : \right. \\
& + \sum_{n=2}^{\infty} (i)^n f_{ac_1 e_1} \cdots f_{e_{n-1} c_n b} \int d^4 s_1 \cdots d^4 s_n : \mathbf{A}^{c_1}(s_1) \cdot \mathbf{p} \cdots \mathbf{A}^{c_n}(s_n) \cdot \left[\mathbf{p} - \sum_1^{n-1} \mathbf{s}_i \right] : \\
& \quad \times \frac{d}{dg} \left[g^{n+1} D(\mathbf{p}) D(\mathbf{p} - \mathbf{s}_1) \cdots D \left[\mathbf{p} - \sum_1^n \mathbf{s}_n \right] \right] \\
& \quad \left. \times \delta \left[\mathbf{p} + \mathbf{k} - \sum_1^n \mathbf{s}_i \right] \delta \left[x - \sum_1^n s_{i0} \right] \right\}. \tag{B5}
\end{aligned}$$

The Feynman rules used here are based on this expansion. The general structure of the n th term is a Coulomb line with $n + 1$ segments. One of the segments is infrared singular, $F(\mathbf{p})$, and others are nonsingular, $D(\mathbf{p})$. The singular Coulomb propagator occurs in $n + 1$ different locations. When external gluons are attached, the modified Coulomb interaction in S_I has the form shown in Fig. 7(c). The external gluons at either end can be replaced by quarks.

APPENDIX C: INFRARED-SINGULAR LIMITS

Consider an arbitrary Feynman diagram with G internal gluon lines (of any type), Q quark lines, F singular Coulomb lines, and D nonsingular Coulomb lines. The number of vertices of each type is specified by n_α , where α indicates the particles coupled. If there are L momentum loops, the amplitude corresponding to a given diagram is of order λ^M , where

$$M = F + L - G - Q. \tag{C1}$$

The number of loops is related to the number of lines and the number of vertices of all types.

$$L = 1 + G + Q + F + D - \sum_{\alpha} n_{\alpha}. \tag{C2}$$

If there are no external Coulomb lines of either type,

$$2F = n_{ggF} + n_{qqF} + n_{FgD}, \tag{C3a}$$

$$2D = n_{FgD} + 2n_{DgD} + n_{ggD} + n_{qqD}. \tag{C3b}$$

Equations (C2) and (C3) can be used to write M in terms of the number of vertices of each type.

The approximation is justified by the goal of identifying the dominant contributions in the zero-momentum limit.

The operator of interest is $F_{ab} = d[gD_{ab}]/dg$. When the n th term of (B1), with $1/p^2 \rightarrow D(\mathbf{p})$, is multiplied by g , there are $n + 1$ factors of $D(\mathbf{p}_i)$ and $n + 1$ powers of g . Thus, the operator expansion for the Coulomb interaction is

$$M = 1 - n_{gggg} - n_{ggg} - n_{qqg}. \tag{C4}$$

The identity

$$n_{FgD} = n_{ggD} + n_{qqD}, \tag{C5}$$

led to additional cancellations in (C4). This last relation is derived from the observation that a single Coulomb line couples at the ends to either two gluons or two quarks. The Coulomb line is segmented into VEV's of Coulomb operators separated by vertices with gluon emission. (See Appendix B.) The linearity of the relationship $F = d[gD]/dg$ means that only one segment along a line is F type and all the rest are D type. If the F segment is at the end of the line, then for that line $n_{FgD} = 1 = n_{ggD} + n_{qqD}$. If the F segment is in the middle, the $n_{FgD} = 2 = n_{ggD} + n_{qqD}$. Thus, (C5) holds for each internal Coulomb line and for a complete diagram with an arbitrary number of Coulomb lines.

APPENDIX D: RENORMALIZATION

Divergences in the integrals of Sec. III are absorbed into seven renormalization constants and the quark mass. The seven constants are defined by $D(\mathbf{p}) = Z_D D_R(\mathbf{p})$, $F(\mathbf{p}) = Z_F F_R(\mathbf{p})$, $A(\mathbf{p}) = Z_A R_R(\mathbf{p})$, $g = Z_g g_R$, $1 + G_1(\mathbf{p}) = Z_1 [1 + G_{1R}(\mathbf{p})]$, $1 + G_2(\mathbf{p}) = Z_2 [1 + G_{2R}(\mathbf{p})]$, and $g' = Z_g g'_R$. A distinction is made between the gluon-gluon-Coulomb coupling constant g and the quark-quark-Coulomb constant g' . They are equal in lowest order, but their renormalization differs by a finite, calculable factor.

The subtracted and renormalized version of (3.1) is

$$Z_D D_R(k) = \frac{1}{k^2} [1 - Z_g^2 Z_A Z_D g_R I_R(\nu)]^{-1} \left[1 - \frac{Z_g^2 Z_A Z_D}{1 - Z_g^2 Z_A Z_D g_R I_R(\nu)} g_R [I_R(k) - I_R(\nu)] \right]^{-1}. \quad (D1)$$

If

$$Z_D = 1 + g_R I_R(\nu) \quad (D2)$$

and

$$Z_g^2 Z_D^2 Z_A = 1, \quad (D3)$$

Eq. (D1) becomes

$$g_R D_R(k) = \frac{g_R}{k^2 \{1 - g_R [I_R(k) - I_R(\nu)]\}}. \quad (D4)$$

When the running coupling constant $g(k) = k^2 g_R D_R(k)$ is introduced, (D4) is equivalent to

$$\frac{1}{g(k)} = \frac{1}{g_R} - [I_R(k) - I_R(\nu)], \quad (D5)$$

and $g_R = g(\nu)$. Equation (3.21a) is the result of subtracting (D5) once more at $\mathbf{k} = 0$.

The renormalization of (3.4) for $F(k)$ proceeds in the same way:

$$Z_F F_R(k) = k^2 D(k)^2 [1 + g^2 J(k)] = \frac{Z_D^2}{k^2} \frac{g(k)^2}{g_R^2} [1 + Z_g^2 Z_A Z_F g_R^2 J_R(\nu)] \times \left[1 + \frac{Z_g^2 Z_A Z_F}{1 + Z_g^2 Z_A Z_F g_R^2 J_R(\nu)} g_R^2 [J_R(k) - J_R(\nu)] \right]. \quad (D6)$$

The choice

$$Z_F = Z_D^2 [1 + Z_g^2 Z_A Z_F g_R^2 J_R(\nu)], \quad (D7)$$

converts (D6) into (3.21b).

Two subtractions are needed to render finite the F_2 integral in (3.15). This is accomplished by writing (3.15) in the form

$$\frac{1 + \bar{F}_1(\nu) + [\bar{F}_1(k) - \bar{F}_1(\nu)]}{A(k)^2} - \frac{1 + \bar{F}_1(\nu) + [\bar{F}_1(k) - \bar{F}_1(p)]}{A(p)^2} = (k^2 - p^2) \left[1 + \frac{\bar{F}_2(\nu) - \bar{F}_2(p)}{\nu^2 - p^2} \right] + \bar{F}_2(k) - \bar{F}_2(p) - \frac{k^2 - p^2}{\nu^2 - p^2} [\bar{F}_2(\nu) - \bar{F}_2(p)]. \quad (D8)$$

Next renormalization constants are introduced and the subtraction momentum p is set equal to zero:

$$\frac{1 + Z_g^2 Z_F Z_A \bar{F}_{1R}(\nu)}{Z_A^2} \left[\frac{1 + f_1 [\bar{F}_{1R}(k) - \bar{F}_{1R}(\nu)]}{A(k)^2} - \frac{1 + f_1 [\bar{F}_{1R}(0) - \bar{F}_{1R}(\nu)]}{A(0)^2} \right] = \left[1 + \frac{Z_g^2 Z_F}{Z_A} \frac{\bar{F}_{2R}(\nu) - \bar{F}_{2R}(0)}{\nu^2} \right] \left[k^2 + f_2 [\bar{F}_{2R}(k) - \bar{F}_{2R}(0)] - \frac{k^2}{\nu^2} [\bar{F}_{2R}(\nu) - \bar{F}_{2R}(0)] \right], \quad (D9)$$

where

$$f_1 = \frac{Z_g^2 Z_F Z_A}{1 + Z_g^2 Z_F Z_A \bar{F}_{1R}(\nu)}, \quad (D10a)$$

$$f_2 = \frac{Z_g^2 Z_F / Z_A}{1 + \frac{Z_g^2 Z_F}{Z_A} \frac{\bar{F}_{2R}(\nu) - \bar{F}_{2R}(0)}{\nu^2}}. \quad (D10b)$$

Using the conditions

$$Z_A^2 = \frac{1 + Z_g^2 Z_F Z_A \bar{F}_{1R}(\nu)}{1 + \frac{Z_g^2 Z_F}{Z_A} \frac{\bar{F}_{2R}(\nu) - \bar{F}_{2R}(0)}{\nu^2}} \quad (D11)$$

and

$$1 = \frac{Z_g^2 Z_F Z_A}{1 + Z_g^2 Z_F Z_A \bar{F}_{1R}(\nu)}, \tag{D12}$$

one finds $f_1 = f_2 = 1$, and (D9) becomes (3.21c). Equation (D12) is compatible with (D2), (D3), and (D7) if the divergent parts of $J_R(\nu)$ and $F_{1R}(\nu)$ are equal. The condition on the renormalizability of the mean-field model is satisfied. The coupling constants at the DgD and ggF vertices remain equal after renormalization. In addition, Z_A is finite.

Quark propagators are renormalized in a similar way. Equation (3.19) takes on the form

$$Z_1 [1 + \bar{G}_{1R}(k)] = [1 + Z_F Z_g^2 IG_{1R}(\nu)] \times \{1 + g_1 [IG_{1R}(k) - IG_{1R}(\nu)]\}, \tag{D13a}$$

$$Z_2 [1 + \bar{G}_{2R}(k)] = \left[1 + \frac{Z_F Z_g^2 Z_2}{Z_1} I\bar{G}_{2R}(\nu)\right] \times \{1 + g_2 [I\bar{G}_{2R}(k) - I\bar{G}_{2R}(\nu)]\}, \tag{D13b}$$

where

$$g_1 = \frac{Z_F Z_g^2}{1 + Z_F Z_g^2 IG_{1R}(\nu)}, \tag{D14a}$$

$$g_2 = \frac{Z_F Z_g^2 Z_2 / Z_1}{1 + \frac{Z_F Z_g^2 Z_2}{Z_1} IG_{2R}(\nu)}, \tag{D14b}$$

and $IG_i(k)$ stands for the integrals on the right-hand side of (3.19). One of the factors in the integrand is the infrared-finite quark energy function

$$\begin{aligned} \bar{E}(s) &= Z_1 [s^2 (1 + \bar{G}_{1R})^2 + m_R^2 (1 + \bar{G}_{2R})^2]^{1/2} \\ &= Z_1 \bar{E}_R(s). \end{aligned} \tag{D15}$$

The renormalized quark mass is $m_R = (Z_1 / Z_2) m = \frac{4}{3} m$. If

$$Z_1 = 1 + Z_F Z_g^2 IG_{1R}(\nu), \tag{D16a}$$

$$Z_2 = 1 + \frac{Z_F Z_g^2 Z_2}{Z_1} IG_{2R}(\nu), \tag{D16b}$$

$$Z_F Z_g^2 = Z_1, \tag{D16c}$$

all divergences cancel, $g_1 = g_2 = 1$, and (D13) becomes (3.24).

The divergences in the various integrals can be analyzed with dimensional regularization. Poles appear at $d = 3$ dimensions. Certain ratios of renormalization constants are finite. In particular

$$\begin{aligned} Z_g^2 / Z_g'^2 &= \frac{1 - IG_{1R}(\nu)}{\left[[1 - F_{1R}(\nu)] \left[1 - \frac{F_{2R}(\nu) - F_{2R}(0)}{\nu^2} \right] \right]^{1/2}} \\ &= \left[\frac{5}{3} \right]^{1/2} \frac{N^2 - 1}{2N^2}. \end{aligned} \tag{D17}$$

The quark and gluon couplings to a Coulomb line differ by a finite factor after renormalization, a consequence of the suppression of certain diagrams. (When $N = 3$, $Z_g^2 / Z_g'^2 = 0.57$.) In order to recover the results of conventional QCD renormalization, one must hold the divergent constant $\lambda(\mu)$ fixed both for the p_0 integrations and also for renormalization. Only after renormalization should the $\lambda \rightarrow \infty$ limit be taken. The missing diagrams are not expected to make finite contributions to any amplitudes.

APPENDIX E: CORRECTIONS

Perturbation theory in the mean-field model is simplified by the elimination of quark and gluon self-energies and the suppression of certain vertices. The price of that simplification is a nonlocal Coulomb interaction. The derivation of the self-consistency equations required, as a practical matter, a number of approximations. In particular calculations in the effective field theory were carried out to order g^2 . Section VI and this appendix are devoted to a discussion of a variety of higher-order diagrams.

The operator-product expansions for the Green's function and the modified Coulomb interaction were simplified by the neglect of vertex corrections at the points where gluons are emitted from a Coulomb line. Figure 6(a) shows the first correction to a point vertex. If a gluon of momentum $p + k$ is emitted by a D -line carry-

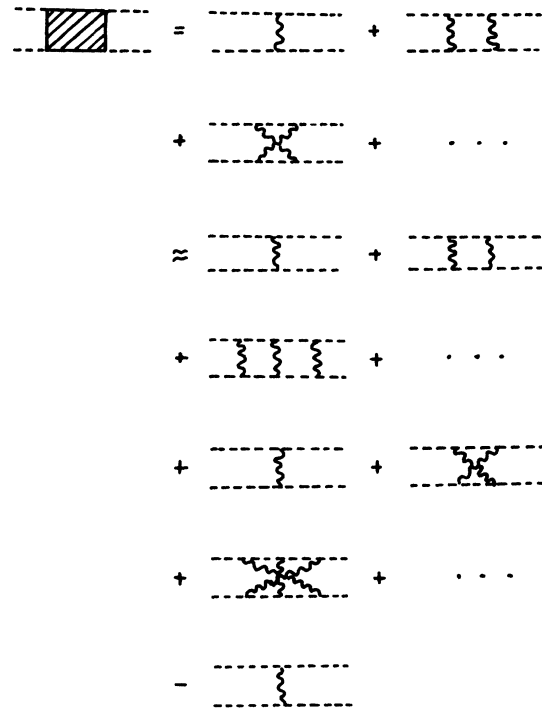


FIG. 8. Two D -type Coulomb lines interact by gluon exchange. The ladder diagrams and crossed ladder diagrams are separately summed to produce Bethe-Salpeter-type wave functions.

ing momentum \mathbf{p} , the factor $\mathbf{A}(\mathbf{p}+\mathbf{k})\cdot\mathbf{p}$ is replaced by $\mathbf{A}(\mathbf{p}+\mathbf{k})\cdot[\mathbf{p}+\Gamma(\mathbf{p},\mathbf{k})]$ where

$$\Gamma_i(\mathbf{p},\mathbf{k}) = -\alpha \int d^3s D(\mathbf{p}-\mathbf{s})D(-\mathbf{k}-\mathbf{s})\mathbf{p}\cdot P(\mathbf{s})\cdot\mathbf{k} \\ \times \mathbf{A}(s)(\mathbf{p}-\mathbf{s})_i. \quad (\text{E1})$$

The integral is convergent; no ultraviolet renormalization is necessary. There are no infrared singularities. The infrared limit of (E1) is obtained by scaling all momenta by a common factor γ and using the infrared limits of $D(s) \propto s^{-5/2}$ and $A(s) \propto s^0$. One finds that both the point vertex term p_i and Γ_i are of order γ . Hence, the use of (E1) in the operator-product expansion makes no qualitative change in infrared or ultraviolet properties.

Figure 6(b) depicts a generic higher-order contribution to $\Gamma_i(\mathbf{p},\mathbf{k})$. Simple power counting for a diagram with N internal gluons and $2N$ internal D -lines shows that there are no ultraviolet divergences in any order. The scaling argument indicates that the infrared limits of $D(s)$ and $A(s)$ are matched so that $\Gamma_i \propto \gamma$ in any order. Moreover, as a vector, $\Gamma_i(\mathbf{p},\mathbf{k})$ is proportional to a linear combination of the vectors \mathbf{p} and \mathbf{k} . In the limit $\mathbf{p} \rightarrow 0$,

$\mathbf{A}(\mathbf{p}+\mathbf{k})\cdot\Gamma(\mathbf{p},\mathbf{k})$ vanishes. There is as much infrared suppression from the full vertex function as there is from a point vertex. Thus, on the assumption that higher order in g^2 means smaller, the neglect of vertex corrections in the operator-product expansion is justified.

Smallness of finite higher-order corrections can be tested with Fig. 6(c). One has a vertex insertion in the integral $I(k)$ used in (3.1) and (3.2) to calculate $D(k)$. Numerical evaluation is necessary. Consistent with the scaling behavior of the vertex, there is no change in the $\mathbf{k} \rightarrow 0$ power dependence of $D(k)$. If $D(k) \simeq \eta k^{-5/2}$, then (3.21a) leads to a condition of the form $1 = \eta^2 I_0$. The vertex correction changes this to $1 = \eta^2 I_0 + \eta^4 I_1 \simeq \eta^2 I_0 (1 + I_1/I_0^2) = \eta^2 I_0 (1 + 0.11)$. There is a 5% shift in the coefficient η .

The full operator-product expansion for $F_{ab}(\mathbf{p},\mathbf{k};x)$ was not used in the calculation of effective propagator functions. Two gluon terms in the expansion produce the g^4 corrections to the gluon self-energy shown in Figs. 6(e)–6(h). Unlike diagrams with three-gluon, four-gluon, or quark-quark-gluon vertices, these contributions do not vanish in the infrared limit. The gluonic corrections to $F_1(k)$ and $F_2(k)$ are

$$F_1^{(4)}(k) = \frac{\alpha^2}{4} \int d^3s d^3t A(s)A(t)[(\mathbf{k}-\mathbf{s})\cdot P(\mathbf{t})\cdot P(\mathbf{k})\cdot P(\mathbf{s})\cdot(\mathbf{k}+\mathbf{t})] \frac{1}{g^2} \frac{d}{dg} [g^3 D(\mathbf{k}+\mathbf{t})D(\mathbf{k}+\mathbf{t}-\mathbf{s})D(\mathbf{k}-\mathbf{s})] \quad (\text{E2})$$

and

$$F_2^{(4)}(k) = \frac{\alpha^2}{2} \int d^3s d^3t [A(s)/A(t) - 1] \text{tr}[P(\mathbf{s})\cdot P(\mathbf{t})][(\mathbf{s}+\mathbf{t})\cdot P(\mathbf{k})\cdot(\mathbf{s}+\mathbf{t})] \frac{1}{g^2} \frac{d}{dg} [g^3 D(\mathbf{s}+\mathbf{t})^2 D(\mathbf{s}+\mathbf{t}+\mathbf{k})] \\ + \alpha^2 \int d^3s d^3t \frac{A(s)}{A(t)} [(\mathbf{t}-\mathbf{k})\cdot P(\mathbf{s})\cdot P(\mathbf{t})\cdot P(\mathbf{k})\cdot(\mathbf{s}+\mathbf{t})] \frac{1}{g^2} \frac{d}{dg} [g^3 D(\mathbf{k}-\mathbf{t})D(\mathbf{k}-\mathbf{t}-\mathbf{s})D(-\mathbf{t}-\mathbf{s})]. \quad (\text{E3})$$

The quark loop diagram of Fig. 6(h) adds to (E3) but is suppressed by a power of N . The coupling constant derivative generates the singular function $F(k)$ through $F = d[gD]/dg$. In each integral there are factors that eliminate the δ function in $F(\mathbf{k}) \simeq \lambda \delta^3(k)$, and there are no manifest infrared singularities in (E2) or (E3). For comparison the lowest-order terms in (3.11) are singular. A scaling argument indicates that (E2) and (E3) have the same $k \rightarrow 0$ behavior as (3.11). Hence, the higher-order terms in the operator-product expansion of $F_{ab}(\mathbf{p},\mathbf{k};x)$ do not generate singularities but rather produce finite, higher-order corrections.

APPENDIX F: BETHE-SALPETER EQUATION FOR D -TYPE COULOMB LINES

The modified Coulomb interaction is defined in terms of a particular integral (2.19) of the product of two modified Coulomb Green's functions. Direct calculation of the VEV of the interaction requires the ability to calculate the VEV of the product of two Green's functions. In addition, to understand the anomalous interactions, one must compute the VEV of products of Green's functions and/or modified interactions. Consider the quantity

$$\delta(z)H_{cd}^{ab}(\mathbf{p},\mathbf{k};\mathbf{q},\mathbf{r}) = (2\pi)^6 \int dx dy \delta(z+y-z) \langle D_{ab}(\mathbf{p},\mathbf{k};x)D_{cd}(\mathbf{q},\mathbf{r};y) \rangle. \quad (\text{F1})$$

When the operator-product expansion of Appendix B (with point vertices) is used for $D_{ab}(\mathbf{p},\mathbf{k};x)$, one is faced with summing the diagrams of Fig. 8. The two Coulomb lines interact with each other via gluon exchange. What is needed is the Bethe-Salpeter equation for Green's-function–Green's-function scattering. In the ladder approximation the two contributing amplitudes are related by crossing:

$$\delta(z)H_{cd}^{ab}(\mathbf{p},\mathbf{k};\mathbf{q},\mathbf{r}) = \delta_{ab}\delta_{cd}\delta(\mathbf{p}+\mathbf{k})\delta(\mathbf{q}+\mathbf{r})D(\mathbf{p})D(\mathbf{q})\delta(z) \\ + \int dx dy \delta(x+y-z) \{ \Phi_{cd}^{ab}(\mathbf{p},\mathbf{q};\mathbf{k},\mathbf{r};x,y) + \Phi_{dc}^{ab}(\mathbf{p},\mathbf{r};\mathbf{k},\mathbf{q};x,y) - \Phi_{0cd}^{ab}(\mathbf{p},\mathbf{q};\mathbf{k},\mathbf{r};x,y) \}. \quad (\text{F2})$$

The single-gluon-exchange amplitude is

$$\begin{aligned} \int dx dy \delta(x+y-z) \Phi_{0cd}^{ab}(\mathbf{p}, \mathbf{k}; \mathbf{q}, \mathbf{r}; x, y) \\ = -\delta(z) \frac{\alpha}{N} f_{aeb} f_{ced} D(\mathbf{p}) D(\mathbf{k}) D(\mathbf{q}) D(\mathbf{r}) \mathbf{p} \cdot \mathbf{P}(\mathbf{p} + \mathbf{k}) \cdot \mathbf{q} A(\mathbf{p} + \mathbf{k}) \delta^3(p+k+q+r). \end{aligned} \quad (\text{F3})$$

Since Φ_0 is common to both ladder amplitudes, it is subtracted to avoid double counting.

A general ladder diagram has both colored and color-singlet components. Only the color-singlet component is expected to produce an enhanced infrared singularity. When the singlet part is projected out,

$$\int dx dy \delta(x+y-z) \Phi_{cd}^{ab}(\mathbf{p}, \mathbf{q}; \mathbf{k}, \mathbf{r}; x, y) = \frac{\delta_{ac} \delta_{bd}}{N^2 - 1} \delta(z) D(\mathbf{p}) D(\mathbf{q}) D(\mathbf{k}) D(\mathbf{r}) \delta(\mathbf{p} + \mathbf{k} + \mathbf{q} + \mathbf{r}) \Psi \left[\frac{\mathbf{p} - \mathbf{q}}{2}, -\frac{\mathbf{k} - \mathbf{r}}{2}; \frac{\mathbf{p} + \mathbf{q}}{2} \right], \quad (\text{F4})$$

and $\Psi(\mathbf{s}, \mathbf{t}; \mathbf{E})$ is a three-dimensional Bethe-Salpeter wave function. The integral equation is

$$\Psi(\mathbf{s}, \mathbf{t}; \mathbf{E}) = \alpha A(\mathbf{s} - \mathbf{t})(\mathbf{s} - \mathbf{E}) \cdot \mathbf{P}(\mathbf{s} - \mathbf{t}) \cdot (\mathbf{s} + \mathbf{E}) + \alpha \int d^3 u D(\mathbf{E} + \mathbf{u}) D(\mathbf{E} - \mathbf{u})(\mathbf{s} - \mathbf{E}) \cdot \mathbf{P}(\mathbf{s} - \mathbf{u}) \cdot (\mathbf{s} + \mathbf{E}) A(\mathbf{s} - \mathbf{u}) \Psi(\mathbf{u}, \mathbf{t}; \mathbf{E}). \quad (\text{F5})$$

The VEV of $F_{ab}(\mathbf{p}, \mathbf{k}; z)$ is proportional to the infrared singular function $F(\mathbf{k})$, where

$$\begin{aligned} F(\mathbf{k}) \delta(\mathbf{p} + \mathbf{k}) \delta_{ad} = \int d^3 s s^2 H_{bd}^{ab}(\mathbf{p}, \mathbf{s}; -\mathbf{s}, \mathbf{k}) \\ = \delta_{ad} \delta(\mathbf{p} + \mathbf{k}) D(\mathbf{k})^2 \left\{ k^2 + \int d^3 s D(\mathbf{s})^2 \left[\frac{1}{N^2 - 1} \Psi \left[\frac{-\mathbf{k} + \mathbf{s}}{2}, \frac{\mathbf{k} - \mathbf{s}}{2}; -\frac{\mathbf{k} + \mathbf{s}}{2} \right] \right. \right. \\ \left. \left. + \Psi(-\mathbf{k}, -\mathbf{s}; 0) - \frac{1}{N^2 - 1} \alpha \mathbf{k} \cdot \mathbf{P}(\mathbf{s} - \mathbf{k}) \cdot \mathbf{k} A(\mathbf{s} - \mathbf{k}) \right] \right\}. \end{aligned} \quad (\text{F6})$$

Retaining just those terms which survive the $N \rightarrow \infty$ limit, one finds

$$F(\mathbf{k}) = D(\mathbf{k})^2 [k^2 + \Psi(\mathbf{k})], \quad (\text{F7})$$

where

$$\begin{aligned} \Psi(\mathbf{k}) &\equiv \int d^3 s D(\mathbf{s})^2 \Psi(-\mathbf{k}, -\mathbf{s}; 0) \\ &= \alpha \int d^3 s D(\mathbf{s})^2 \mathbf{k} \cdot \mathbf{P}(\mathbf{s} - \mathbf{k}) \cdot \mathbf{k} A(\mathbf{s} - \mathbf{k}) + \alpha \int d^3 u D(\mathbf{u})^2 \mathbf{k} \cdot \mathbf{P}(\mathbf{k} - \mathbf{u}) \cdot \mathbf{k} A(\mathbf{u} - \mathbf{k}) \Psi(\mathbf{u}). \end{aligned} \quad (\text{F8})$$

When (F7) is used to write $\Psi(\mathbf{k})$ in terms of $F(\mathbf{k})$, the integral equation for $\Psi(\mathbf{k})$ becomes (3.4), the integral equation for $F(k)$.

This alternate derivation of (3.4) is useful because it suggests that the singularity in $F(\mathbf{k})$ arises from the binding of two D -type Coulomb lines by gluon exchange. Since there is no need to compute the derivative with respect to coupling constant of unknown functions, it is easier in this approach to identify possible corrections to $F(\mathbf{k})$. Approximations that could be improved are the ladder approximation, the restriction to color-singlet configurations, and the use of point vertices.

APPENDIX G: WARD IDENTITIES

In a gauge theory the Ward identities provide a system of constraint equations that can be used to prove the renormalizability of the theory. Unfortunately, the standard identities¹⁹ cannot be used in the Coulomb gauge when the theory is quantized in Hamiltonian form. However, there should still be a conserved color current $J_\mu^a(x)$, and one can use old-fashioned methods. If one ignores all subtleties about canonical quantization, there exists the identity

$$\partial_\mu \langle 0 | T [J_\mu^a(x) \psi_\alpha(y) \bar{\psi}_\beta(z)] | 0 \rangle = \langle 0 | T \{ [J_\mu^a(x), \psi_\alpha(y)] \delta(x_0 - y_0) \bar{\psi}_\beta(z) + \psi_\alpha(y) [J_\mu^a(x), \bar{\psi}_\beta(z)] \delta(x_0 - y_0) \} | 0 \rangle. \quad (\text{G1})$$

The equal-time commutator on the right can be evaluated with canonical commutation rules. In the Coulomb gauge the current can be identified from $\partial_\mu F_a^{\mu\nu} = g J_a^\nu$. Gauss's law is used to eliminate $A_0^a(x)$. $F_a^{0i}(x)$ is replaced by the canonical momentum field $P_i^a(x)$ and a longitudinal term involving the modified Coulomb interaction. The result is that $J_0^a(x)$ becomes

$$J_0^a(x) = -\nabla^2 \int d^3 y D_{ab}(\mathbf{x}, \mathbf{y}; x_0) K_0^b(\mathbf{y}, x_0), \quad (\text{G2})$$

where $K_0^b(z) = \bar{\psi}(z) \gamma_0 (\lambda_b / 2) \psi(z) - f_{bcd} \mathbf{P}_c(z) \cdot \mathbf{A}_d(z)$. The left-hand side of (G1) is complicated by the structure of the spatial part of the color current:

$$\begin{aligned}
J_a^i(x) = & \bar{\psi}(x)\gamma^i \frac{\lambda_a}{2} \psi(x) + f_{abc} \epsilon_{ist} A_s^b(x) B_t^c(x) + g f_{abc} \int d^3y F_{bd}(\mathbf{x}, \mathbf{y}; x_0) K_0^d(\mathbf{y}, x_0) P_c^i(x) \\
& - g^2 f_{abc} \int d^3y F_{bd}(\mathbf{x}, \mathbf{y}; x_0) K_0^d(\mathbf{y}, x_0) \nabla_i \int d^3z D_{ce}(\mathbf{x}, \mathbf{z}; x_0) K_0^e(\mathbf{z}, x_0) .
\end{aligned} \tag{G3}$$

If one makes a drastic approximation and replaces each Coulomb function by its VEV and transforms to momentum space, the Ward identity becomes

$$\begin{aligned}
\frac{ip^2 D(\mathbf{p})}{(2\pi)^8} \delta^4(q+p+k) & \left[\frac{\lambda_a}{2} S(-k) - S(q) \frac{\lambda_a}{2} \right] \\
= & -ip_0 p^2 D(p) \langle 0 | K_0^a(p) \psi_\alpha(q) \bar{\psi}_\beta(k) | 0 \rangle \\
& + ip_i \left\langle 0 \left| \int d^4s \left[\bar{\psi}(s) \gamma^i \frac{\lambda_a}{2} \psi(p-s) + f_{abc} \epsilon_{ist} A_s^b(s) B_t^c(p-s) \right] + g f_{abc} \int d^4s F(\mathbf{s}) K_0^b(s) P_c^i(p-s) \right. \right. \\
& \left. \left. - g^2 f_{abc} \int d^4s F(\mathbf{s}) K_0^b(s) [i(p-s)_i D(p-s)] K_0^e(p-s) \right] \psi_\alpha(q) \bar{\psi}_\beta(k) \right| 0 \rangle ,
\end{aligned} \tag{G4}$$

where $S(k)$ is the fermion propagator from (2.16) and

$$K_0^b(s) = \int d^4t \left[\bar{\psi}(t) \gamma^0 \frac{\lambda_b}{2} \psi(s-z) - f_{bgh} \mathbf{P}_g(t) \cdot \mathbf{A}_h(s-t) \right] . \tag{G5}$$

This is still too complicated to evaluate explicitly.

The interesting question is to what extent the assumption of an infrared singularity is consistent with this Ward identity. The singularity does not cancel in the difference of quark propagators on the left-hand side of (G4). The fourth term on the right is of order $g^2\lambda$, where $F(\mathbf{s}) \approx \lambda \delta^3(\mathbf{s})$. Keeping just that term on the right and working in lowest order, I find

$$\frac{\alpha' \lambda}{2} \left[\frac{\boldsymbol{\gamma} \cdot [\mathbf{q}] + \bar{m}(\mathbf{q})}{\bar{E}(\mathbf{q})} - \frac{\boldsymbol{\gamma} \cdot [-\mathbf{k}] + \bar{m}(-\mathbf{k})}{\bar{E}(-\mathbf{k})} \right] = \frac{g^2 N}{4(2\pi)^3} \lambda \frac{\lambda_a}{2} \left[\frac{\boldsymbol{\gamma} \cdot [\mathbf{q}] + \bar{m}(\mathbf{q})}{\bar{E}(\mathbf{q})} - \frac{\boldsymbol{\gamma} \cdot [-\mathbf{k}] + \bar{m}(-\mathbf{k})}{\bar{E}(-\mathbf{k})} \right] , \tag{G6}$$

where $[\mathbf{q}] = \mathbf{q}[1 + G_1(\mathbf{q})]$ and $\bar{m}(\mathbf{q}) = m[1 + G_2(\mathbf{q})]$. The fortuitous result is that the two sides are equal except for the fact that α' contains a factor of $(N-1)/N$ while a simple N appears on the right. The Ward identity is consistent with the hypothesized infrared singularity, at least in the $N \rightarrow \infty$ limit.

The agreement with the Ward identity is surprising since the current densities in (G2) do not satisfy the standard commutation rules. An equivalent gluonic calculation is likely to be less successful. The anomalous interactions become important. Moreover, it is likely that additional terms are needed in (G2) and (G3) to preserve current conservation. What is needed is a Hamiltonian based statement of the symmetry that can be used to derive Ward identities consistent with Hamiltonian quantization.

Two final comments are in order. The infrared singular term on the right-hand side of (G4) is longitudinal. It is proportional to p_i and does not contribute to the quark-quark-gluon vertex function. In addition, the assumptions in this paper about the VEV's of operators probe the structure of the vacuum state. Although the assumptions are self-consistent within QCD, they may reflect some sort of spontaneous symmetry breaking on the part of the vacuum state. In that case there may be no Ward identities based on a conserved current.

APPENDIX H: WILSON LOOP

A typical term in the expansion of the VEV in (4.6) has the form

$$\begin{aligned}
L_{nm} = & (i)^{n+m} \text{tr}(\lambda^{a_1} \cdots \lambda^{a_n} \lambda^{b_1} \cdots \lambda^{b_m}) \left[\int_0^T dy_1 \int_0^{y_1} dy_2 \cdots \int_0^{y_{n-1}} dy_n \right] \left[\int_T^0 dx_1 \int_T^{z_1} dz_1 \cdots \int_T^{z_{m-1}} dz_m \right] \\
& \times \langle A_4^{a_1}(\mathbf{nR}, y_1) \cdots A_4^{a_n}(\mathbf{nR}, y_n) A_4^{b_1}(0, z_1) \cdots A_4^{b_m}(0, z_m) \rangle .
\end{aligned} \tag{H1}$$

A contraction between adjacent fields on one side of the loop yields

$$\int_0^{y_{i-1}} dy_i \int_0^{y_i} dy_{i+1} \int_0^{y_{i+1}} dy_{i+2} \lambda_{is}^{a_i} \lambda_{sj}^{a_{i+1}} \langle A_4^{a_i}(\mathbf{nR}, y_i) A_4^{a_{i+1}}(\mathbf{nR}, y_{i+1}) \rangle = \frac{2(N^2-1)}{N} \delta_{ij} \frac{1}{2} V(0) \int_0^{y_{i-1}} dy_i \int_0^{y_i} dy_{i+2} . \tag{H2}$$

The λ^a matrices satisfy $(\lambda^a \lambda^a)_{ij} = [2(N^2-1)/N] \delta_{ij}$. The chain of ordered integrals along a side is shortened by one for

each adjacent pair contraction. The integral that marks the position of the contraction is empty in the sense that its argument is unity. Contractions along a side of the loop that are not between adjacent fields vanish due to the conflict between time ordering and the instantaneous propagator.

The multiple integral over z_1, \dots, z_m in (H1) is reordered:

$$\int_T^0 dz_1 \int_T^{z_1} dz_2 \cdots \int_T^{z_{m-1}} dz_m = (-1)^m \int_0^T dz_m \int_0^{z_m} dz_{m-1} \cdots \int_0^{z_2} dz_1. \quad (\text{H3})$$

Contractions across the loop from $\mathbf{x} = nR$ to $\mathbf{x} = 0$ connect equal times. Since the two sides are time ordered, contractions cannot cross each other. The equal-time propagators are like rungs on a ladder. A generic term in L_{nm} has r rungs, s nearest-neighbor contractions on one side, and t nearest-neighbor contractions on the other side:

$$L_{nm} = (-1)^m (i)^{n+m} N \sum_{s,t} \left[\frac{\rho V(0)}{2} \right]^{s+t} [\rho V(R)]^r I(r,s,t), \quad (\text{H4})$$

where $n = 2s + r$ and $m = 2t + r$. The gauge group factor is $\rho = 2(N^2 - 1)/N$. The residual integral $I(r,s,t)$ includes a sum over all possible orderings of the r rungs, s contractions on one side, and t contractions on the other. Each contraction across the loop from $\mathbf{x} = nR$ to $\mathbf{x} = 0$ produces a factor of $V(R)$. The trace of the product of color matrices collapses to $N\rho^{s+t+r}$. Reordering of the integral in (H3) means that rung contractions are between adjacent pairs of λ matrices in the product in (H1). For example, if $s = t = 0$, equal-time run contractions set $a_n = b_1$, $a_{n-1} = b_2$, etc. When $s \neq 0$ and $t \neq 0$, pairs of adjacent λ matrices are first eliminated by (H2).

Computation of $I(r,s,t)$ begins with a simple example. If $r = 1$, $s = 1$, then the integral on one side has the form

$$\int_0^T dy_1 \int_0^{y_1} dy_2 \int_0^{y_2} dy_3 [F(y_1) + F(y_2) + F(y_3)] = \frac{T^2}{2} \int_0^T F(x) dx. \quad (\text{H5})$$

In general, summing over all possible ordering of s adjacent contractions along a side of length $n = r + 2s$ replaces the original ordered integral by one of length r multiplied by $T^s/s!$. Thus, $I(r,s,t)$ is reduced to

$$I(r,s,t) = \frac{T^s}{s!} \frac{T^t}{t!} I(r,0,0). \quad (\text{H6})$$

The remaining integral $I(r,0,0)$ is

$$I(r,0,0) = \left[\int_0^T dy_1 \cdots \int_0^{y_{r-1}} \right] \left[\int_0^T dw_1 \cdots \int_0^{w_{r-1}} dw_r \right] \delta(y_1 - w_1) \cdots \delta(y_r - w_r) = \frac{T^r}{r!}. \quad (\text{H7})$$

When the various factors are brought together and summed over n and m , the result is (4.8).

- ¹J. Finger, D. Horn, and J. E. Mandula, Phys. Rev. D **20**, 3253 (1979); V. P. Nair and C. Rosenzweig, *ibid.* **31**, 401 (1985); C. Thorn, *ibid.* **19**, 639 (1979); C. Callan, R. Dashen, and D. J. Gross, *ibid.* **17**, 2717 (1978); T. K. Hansson, K. Johnson, and C. Peterson, *ibid.* **26**, 2069 (1982); H. Flyvbjerg, Nucl. Phys. **B176**, 379 (1981).
- ²A. R. Swift and J. L. Rodriguez Marrero, Phys. Rev. D **29**, 1823 (1984).
- ³J. L. Rodriguez Marrero and A. R. Swift, Phys. Rev. D **31**, 917 (1985).
- ⁴J. L. Rodriguez Marrero and A. R. Swift, Phys. Rev. D **32**, 476 (1983).
- ⁵C. M. Bender, T. Eguchi, and H. Pagels, Phys. Rev. D **17**, 1086 (1978); R. Jackiw, I. Muzinich, and C. Rebbi, *ibid.* **17**, 1576 (1978); R. E. Cutkosky, *ibid.* **30**, 447 (1984); R. E. Peccei, *ibid.* **17**, 1987 (1978).
- ⁶B. Foler, H. Nguyen-Quang, and D. Schulte, Phys. Rev. D **34**, 1157 (1986); D. Schulte, *ibid.* **31**, 810 (1985).
- ⁷F. L. Feinberg, Phys. Rev. D **17**, 2659 (1978).
- ⁸K. G. Wilson, Phys. Rev. D **10**, 2445 (1974).
- ⁹A. Chodos, R. L. Jaffe, K. Johnson, C. Thorn, and V. Weisskopf, Phys. Rev. D **9**, 3471 (1974).
- ¹⁰N. H. Christ and T. D. Lee, Phys. Rev. D **22**, 939 (1980).
- ¹¹L. D. Faddeev and V. N. Popov, Phys. Lett. **25B**, 29 (1967); H. Hamber and G. Parisi, Phys. Rev. Lett. **47**, 1792 (1981); D. Weingarten, Phys. Lett. **109B**, 57 (1982).
- ¹²T. D. Lee, *Particle Physics and Introduction to Field Theory* (Harwood Academic, Chur, Switzerland, 1981), Chap. 19.
- ¹³Similar techniques have been used to study spontaneous symmetry breaking: L. N. Chang and N-P. Chang, Phys. Rev. D **29**, 312 (1984); Y. Nambu and G. Jona-Lasinio, Phys. Rev. **122**, 345 (1961).
- ¹⁴J. Schwinger, Phys. Rev. **127**, 324 (1962).
- ¹⁵V. N. Gribov, Nucl. Phys. **B139**, 1 (1978); D. Zwanziger, *ibid.* **B209**, 336 (1982).
- ¹⁶M. Bando, K. Fujii, Y. Abe, T. Okazaki, and S. Kurada, Phys. Rev. D **33**, 548 (1986).
- ¹⁷R. E. Cutkosky, in *Hadron Spectroscopy—1985*, proceedings of the International Conference, edited by S. Oneda (AIP Conf. Proc. No. 132) (AIP, New York, 1985), p. 227.
- ¹⁸The hazards of relying on a particular gauge are exemplified by the original axial gauge model of M. Baker, J. S. Ball, and F. Zachariasen, Nucl. Phys. **B186**, 531 (1981), and the subsequent analysis of G. B. West, Phys. Rev. D **27**, 1878 (1983). The Coulomb gauge has not been subjected to the same kind of scrutiny.
- ¹⁹See, for example, T-D. Cheng and L-F. Li, *Gauge Theory of Elementary Particle Physics* (Clarendon, Oxford, 1984), Sec.

- 9.3.
- ²⁰G. 't Hooft, Nucl. Phys. **B72**, 461 (1974); **B75**, 461 (1974); E. Witten, *ibid.* **B160**, 57 (1979).
- ²¹E. S. Abers and B. W. Lee, Phys. Rep. **9C**, 1 (1973).
- ²²L. S. Brown and W. I. Weisberger, Phys. Rev. D **20**, 3239 (1979).
- ²³A. R. Swift and J. I. Donna, Phys. Rev. D **19**, 657 (1979).
- ²⁴I. Tamm, J. Phys. (Moscow) **9**, 449 (1945); S. M. Dancoff, Phys. Rev. **78**, 382 (1950); F. Dyson, *ibid.* **90**, 994 (1953); **91**, 1543 (1953); J. C. Taylor, *ibid.* **95**, 1313 (1953).
- ²⁵L. S. Celenza and C. M. Shakin, Phys. Rev. D **34**, 1571 (1986); A. Le Yaouanc, L. Oliver, O. Pène, and J-C. Raynal, *ibid.* **29**, 133 (1984).
- ²⁶D. Lurie, *Particles and Fields* (Interscience, New York, 1968), p. 433.
- ²⁷H. Cheng and E-C. Tsai, Phys. Rev. Lett. **57**, 511 (1986).
- ²⁸N. D. Son and J. Sucher, Phys. Rev. **153**, 1496 (1967); B. Silvestre-Brac, A. Bilal, C. Gignoux, and P. Schuck, Phys. Rev. D **29**, 2275 (1984).
- ²⁹M. G. Olsson and C. J. Suchyta, Phys. Rev. D **35**, 1738 (1987).
- ³⁰E. Eichten, K. Gottfried, T. Kinoshita, K. Lane, and T. Yan, Phys. Rev. D **21**, 203 (1980); W. Marciano and H. Pagels, Phys. Rep. **36C**, 137 (1978); L-N. Chang and N-P. Chang, Phys. Rev. D **29**, 312 (1984).